Kendon EJ, Blenkinsop S, Fowler HJ.

When will we detect changes in short-duration precipitation extremes?.

***Journal of Climate* 2018. In Press.**

When will we detect changes in short-duration precipitation extremes?

Elizabeth J. Kendon*

Met Office Hadley Centre, Exeter, UK

Stephen Blenkinsop, Hayley J. Fowler

School of Engineering, Newcastle University, UK

*Corresponding author address: Elizabeth Kendon (nee Kennett), Met Office Hadley Centre, Fitzroy Road, Exeter, EX1 3PB, UK.

Email: elizabeth.kendon@metoffice.gov.uk

Abstract

The question of when we may be able to detect the influence of climate change on UK rainfall extremes is important from a planning perspective, providing a timescale for necessary climate change adaptation measures. Short-duration intense rainfall is responsible for flash flooding, and several studies have suggested an amplified response to warming for rainfall extremes on hourly and sub-hourly timescales. However, there are very few studies examining the detection of changes in sub-daily rainfall. This is due to the high cost of very high-resolution (kilometre-scale) climate models needed to capture hourly rainfall extremes, and to a lack of sufficiently long high-quality sub-daily observational records. Results here using output from a 1.5km climate model over the southern UK indicate that changes in 10-minute and hourly precipitation emerge before changes in daily precipitation. In particular, model results suggest detection times for short-duration rainfall intensity in the 2040s in winter and 2080s in summer, which are respectively 5-10 years and decades earlier than for daily extremes. Results from a new quality-controlled observational dataset of hourly rainfall over the UK do not show a similar difference between daily and hourly trends. Natural variability appears to dominate current observed trends (including an increase in the intensity of heavy summer rainfall over the last 30 years), with some suggestion of larger daily than hourly trends for recent decades. The expectation of the reverse, namely larger trends for short-duration rainfall, as the signature of underlying climate change has potentially important implications for detection and attribution studies.

1. Introduction

Recent UK floods (for example, caused by Storm Angus across the country in November 2016, in the north of the UK in December 2015 and in Somerset in January 2014) have reinforced the need for the UK to gain a better understanding of how its exposure to flooding may change in the future with global warming. This is vital so that appropriate levels of resilience and protection can be delivered through river and land management and investment in flood defences (Cabinet Office & DEFRA, 2016). Short-duration intense rainfall is responsible for flash flooding, important in small, steep catchments and urban areas. Precipitation data at sub-daily scales (down to a few minutes) and spatial scales of 1-10 km^2 are needed for urban drainage design (Arnbjerg-Nielsen et al., 2013) and hence an understanding of changes in precipitation at these scales is important so urban planners can start accounting for the effects of future climate change. Notable UK examples of this type of extreme event were the floods in Boscastle in August 2004 and Newcastle-upon-Tyne in June 2012 (Archer and Fowler, 2015), causing extensive damage and major disruption.

In the context of climate change, with increasing temperature the atmosphere is able to hold more moisture, and this is expected to lead to future increases in heavy rainfall intensity (Trenberth et al., 2003). Further, it has recently been argued that observational evidence of the intensification of extreme rainfall is beginning to show consistency with model studies (Fischer & Knutti, 2016). The Clausius-Clapeyron relation (hereafter referred to as 'CC') suggests that if relative humidity remains constant, atmospheric humidity will increase at a rate that follows the saturation vapour pressure dependency on temperature according to the CC relation – a rate of ~7% per °C of surface warming (e.g. Allen and Ingram, 2002; Pall et al., 2007). This sets a scale for change in precipitation extremes (Trenberth et al., 2003). Several studies have provided observational evidence of a super-CC (2x CC) relationship for hourly (e.g., Lenderink

& van Meijgaard, 2008, 2010, Mishra et al., 2012) and sub-hourly (e.g. Loriaux et al., 2013) extremes which might suggest an amplified response to warming on these timescales. Such super-CC scaling seems to be a property of convective precipitation (Berg et al., 2013), and may be explained by latent heat released within storms invigorating vertical motion, leading to a greater increase in rainfall intensity. The dependency of extreme UK hourly rainfall on temperature has been demonstrated to be consistent with CC scaling in observations (Blenkinsop et al., 2015) and a high resolution, convection-permitting climate model (Chan et al., 2016a) but no evidence has been identified of super-CC scaling, including for simulated 10-minute extremes (Chan et al., 2016b).

Relatively coarse resolution projections (25km) provided by UKCP09 (Murphy et al., 2009) suggest changes in the wettest day of winter (~99th percentile of daily precipitation) range from zero in parts of Scotland to +25% in parts of England (central estimate, 2080s, medium emissions) whilst changes in the wettest day in summer range from –12% in parts of southern England to +12% in parts of Scotland. Summer changes are however subject to high levels of uncertainty associated with the parameterization of convection in these models. Typically, projected changes in sub-daily extremes have been assessed using statistical methods to disaggregate daily precipitation from regional climate models. Darch et al. (2016) used a weather generator to provide illustrative results for 10 UK sites to show a projected increase in the intensity of short-duration events in winter but a reduction in summer. Again, however, these are associated with high uncertainty due to the underlying climate model resolution and the fact that they do not use climate change information at the sub-daily scale. This is being addressed by the new generation of very high resolution, convection-permitting models (CPMs), which explicitly represent convection without the need for a parameterization scheme. These models are able to more realistically represent convection, and to capture hourly rainfall

characteristics including extremes, unlike traditional coarser resolution climate models (Kendon et al., 2012, Chan et al., 2014b). The first CPM climate change simulations for the southern UK project an increased intensity of extreme hourly rainfall in summer and almost a 5-fold increase in events above 30mm/h (a critical accumulation threshold used by the Flood Forecasting Centre to indicate likely flash flooding) (Kendon et al., 2014).

In common with most other parts of the globe, observed long-term variability and detection of trends in UK sub-daily rainfall have received little study due to the lack of sufficiently long, high-quality records (Westra et al., 2014; Hegerl et al., 2015). Faulkner (1999) produced a relatively simple analysis of changes in UK 1h annual maxima, observing a possible decreasing trend over the 20th century but noted that this was potentially subject to inhomogeneities arising from changes in rain gauge type and temporal variations in the observing network. Studies of observed changes in sub-daily rainfall have tended to focus on relatively small regions (with exceptions for the US (Barbero et al., 2017) and Australia (Westra & Sisson, 2011) and show inconsistency in their changes although generally suggest an increase in intensity (Westra et al., 2014). Historical trends in UK daily rainfall have been relatively extensively studied however, identifying more intense winter rainfall since the 1960s (Osborn et al., 2000; Osborn & Hulme, 2002; Maraun et al., 2008) with some evidence of a longer term trend (Osborn et al., 2000; Simpson & Jones, 2014). The contribution to winter rainfall from heavy precipitation events has also increased (Jenkins et al, 2008) whilst Jones et al. (2013) identify increases in seasonal maxima and estimated return frequencies in winter. In contrast, summer rainfall events have shown little change or declined in intensity, whilst longer duration events (multi-day) have increased (Fowler & Kilsby, 2003a,b; Jones et al., 2013). Simpson & Jones (2014) note that trends in mean and extreme summer daily precipitation for regional UK precipitation series (1931-2011) have been mostly negative, whilst Jones et al. (2013) identify spatially

varying changes in the median summer maxima. Although for some regions these events appear to be increasing, in general summer rainfall events have declined in intensity. A recent study (Brown, 2017) has found that these previously reported trends in UK daily rainfall extremes, however, may be due at least in part to natural variability. In particular, the North Atlantic Oscillation (NAO) explains much of the trend in winter extreme rainfall from 1958 to 2012 (with the residual trend after inclusion of NAO much reduced in magnitude and significance), and any apparent trend in summer extreme rainfall.

Evidence of human influence on changes in rainfall has been accumulating globally. For example, Min et al. (2011) showed that human-induced warming has contributed to observed increases in the intensity of heavy precipitation over large parts of Northern Hemisphere land areas. However, the attribution of rainfall trends to human influence on local and regional scales is not yet possible (Sarojini et al., 2016). For some specific extreme events, it is possible to show that anthropogenic climate change increased the risk of the event e.g. the Autumn 2000 floods in England and Wales (Pall et al., 2011) and the 2014 Southern England winter floods (Schaller et al., 2016). However, this is not true of many other flooding events, and it is only with time that we can detect any underlying trend.

An important measure therefore to inform adaptation planning is detection time, i.e. when changes in flooding are expected to move outside of what has been experienced in the past due to natural climate variability. The question of when we may be able to detect the influence of climate change on UK rainfall is examined here. This is important from a planning perspective, providing a timescale for necessary climate change adaptation measures. Detection time is also useful for evaluating climate model projections, as the emergence of the climate change signal predicted by the model can be tested using observations. Fowler & Wilby (2010) examined UK

daily precipitation change from thirteen 50km resolution regional climate model simulations from the PRUDENCE ensemble, and found changes in the winter 10 year return level emerge in the 2040s, whilst changes in summer extremes are highly uncertain. A similar study using the ClimatePrediction.net global climate model ensemble gave similar results (Fowler et al., 2010).

In this paper, we examine how detection time varies for UK precipitation accumulated across a range of time and space scales, including down to 10-minute and kilometre scales, using output from a very high resolution (convection-permitting) climate model and investigate the consistency of modelled detection times with observed changes from gauge data in a new, quality controlled dataset of hourly rainfall for the UK. Convection-permitting models do not necessarily better represent daily precipitation compared to coarser resolution regional climate models (Chan et al., 2013), but are needed to provide reliable projections of sub-daily rainfall and hence an estimate of when we may be able to detect change on these timescales.

2. Data & Methods

a. Climate model

A very high-resolution (1.5km) climate model spanning the southern UK (including most of England and Wales) is used here. This was the largest domain possible to allow completion of decadal length simulations in a reasonable time, and includes regions with different rainfall characteristics. In particular, it includes southern England, where there is a high proportion of convective events in summer; London, where the urban environment has a considerable influence on the local climate; and the mountainous region of Wales, where there is orographic enhancement of rainfall. The model is a modified version of the non-hydrostatic Met Office operational UK variable-resolution model (UKV), a configuration of the Met Office Unified

158 Model (UM) and is described in Kendon et al. (2014). For weather forecasting purposes, 1.5km
159 grid spacing is the finest affordable resolution at which most convection over the UK is
160 satisfactorily represented on the grid without the need for a convection scheme (Lean et al.,
161 2008). Thus in this model, the convection parameterization scheme is switched off. 13-year
162 present- (1996-2009) and future-climate (~2100, RCP8.5 scenario) 1.5-km simulations are
163 driven by a 12km regional climate model (RCM), which spans Europe and is in turn driven by
164 a 60km atmosphere-only general circulation model (GCM). The 12km RCM and 60km GCM
165 both have the UM Global Atmosphere 3.0 configuration (Walters et al., 2011). 10-minute
166 precipitation has been output for the summer months (June-July-August) only, due to the large
167 data volume. Chan et al. (2016b) identified an intensification of these 10-minute extremes that
168 is consistent with that found at hourly timescales, and here we build on these results, examining
169 whether increases in hourly and 10-minute extremes are detectable before changes in daily
170 rainfall extremes.
171
172 The 1.5km model is based on the Met Office operational UK weather forecast model, and
173 extensive testing within numerical weather prediction (NWP) trials indicates that the model
174 produces realistic convective showers and is able to forecast localised extreme events not
175 captured at coarser resolutions (Lean et al., 2008). The 1.5km model has also been shown to
176 realistically capture hourly rainfall in long climate simulations. In particular, Kendon et al.
177 (2012) showed that the model gives a much better representation of the intensity-duration
178 characteristics of hourly rainfall, as well as its spatial extent, compared to a coarser resolution
179 climate model. Kendon et al. (2014) showed the intensity of heavy hourly rainfall and its spatial
180 pattern across the southern UK is well captured in the 1.5km model in both summer and winter;
181 whilst Chan et al. (2014b) showed that the model is more realistic in representing hourly
182 precipitation extremes compared to a 12km climate model. These improvements in the

representation of sub-daily rainfall characteristics are also seen in other CPMs for other regions (Kendon et al., 2017). There is still a tendency for heavy rainfall to be too intense in the 1.5km model, which is a common deficiency in convection-permitting models (Kendon et al., 2017) and likely to be a consequence of convection not being fully resolved at kilometre scales. The model has not been evaluated at sub-hourly timescales from a climatological perspective, due to the lack of UK quality-controlled multi-year sub-hourly observations (Chan et al., 2016b). Focussed field campaigns (e.g. DYMECS project) have shown the 1.5km NWP model does not adequately represent short-lived storm lifecycles, but results vary with the type of convective storms (Stein et al., 2015). We note that 10-minute output corresponds to 12 (50 second) model time steps, and so is approaching the limit imposed by discretisation.

Following Fowler & Wilby (2010), we define a detectable increase in a given precipitation metric D_x as the year at which we would reject (at the α=0.05 or 95% significance level) the null hypothesis that the metric for year x (μ_x) and the control period (1996-2009, μ_c) are equal, in favour of the alternative hypothesis that μ_x is not equal to μ_c. Using a two-tailed test (with critical Z score of 1.96) this corresponds to:

$$|\boldsymbol{D_x}| = \frac{|\boldsymbol{\mu_x} - \boldsymbol{\mu_c}|}{\sqrt{\boldsymbol{\sigma_f^2} + \boldsymbol{\sigma_c^2}}} \geq \mathbf{1.96}$$

where $\boldsymbol{\sigma_c^2}$ ($\boldsymbol{\sigma_f^2}$) is the variance in the metric for the control (future) period. Assuming a linear trend in the metric through time between the present climate simulation (mid-year 2003) and the future simulation (mid-year 2103, metric μ_f), we get the following for the earliest detection year Y_D:

$$\boldsymbol{Y_D} = \mathbf{2003} + \mathbf{196}\frac{\sqrt{\boldsymbol{\sigma_f^2} + \boldsymbol{\sigma_c^2}}}{|\boldsymbol{\mu_f} - \boldsymbol{\mu_c}|}$$

We have used bootstrap resampling to get an estimate of the variance of the metric, due to natural climate variability, in the control and future periods. For each season, we have randomly selected 13 years out of the 13-year period, with replacement, such that in the resampled time series some years occur more than once and other years not at all. By this method, we are retaining any time correlations on sub-seasonal timescales and only assume independence between a given season for one year and the next. This resampling is done identically at each grid point, thus retaining any spatial coherence. The bootstrap resampling procedure is repeated 100 times, for each of the control and future periods. The precipitation metric of interest (μ) is then calculated at each grid point, for each of the bootstrap samples. This allows the detection year Y_D to be calculated at each grid point, using the variance across the 100 estimates of μ for the control and future periods. We finally calculate the median of all the detection times across southern UK land points, to give a single central estimate, as well as the 10^{th} and 90^{th} percentiles of the spatial varying estimates to give an indication of uncertainty.

In this analysis, since we are restricted to single 13-year simulations of the present and future climate, it is not possible to examine initial condition uncertainty. The method of resampling only accounts for year-to-year natural variability, with no consideration of multi-decadal climate variability. The presence of significant multi-decadal variability in the metric could lead to the actual detection time of the climate change signal being earlier or later than that estimated above, depending on where the control and future periods fall within this multi-decadal cycle. We note, however, that given the way the future sea surface temperatures (SSTs) are configured in the driving GCM, we would expect this effect to be small. In particular, the future SSTs are configured as a time-invariant delta (given by the multi-year mean SST change for each month between 1990-2010 and 2090-2110 in HadGEM2-ES) applied onto the present-

day time-varying SSTs (as described in Kendon et al., 2014), and human induced warming (of about 4K globally) is expected to dwarf any influence of natural climate variability in the 20 year mean SST change. Another limitation of the approach here is that it assumes a linear trend in the metric between the control and future periods. In reality, it is likely that changes will start more slowly and then accelerate towards the end of the century, following the projected profile of human-induced warming. This will mean actual detection times are likely to be later than estimated assuming a simple linear trend. Fowler & Wilby (2010) attempted to model this effect by applying a pattern scaling approach, assuming regional changes in precipitation will occur in proportion to the projected change in global mean temperature. In this paper, we just use the simple linear approach, but note this will not impact the finding of whether changes in daily or short-duration precipitation emerge first.

Here we consider three precipitation metrics: i) mean wet day/hour intensity (wet value is >0.1mm per accumulation period); ii) heavy precipitation intensity, defined as the mean of the upper 5% of wet values (p_{95}); and iii) heavy precipitation, defined as the mean of the upper 1% of all values (p_{99ALL}). The precipitation metrics are calculated for 10-minute, hourly and daily precipitation accumulations, using the 13 years of data from the control and future simulations respectively. They are also calculated for the 1.5km precipitation regridded to a range of coarser spatial scales (5km, 12km and 50km) using area-weighted averaging. All temporal-spatial averaging is carried out on the raw precipitation time series data before calculation of the metrics.

b. Change detection in observations

To examine whether evidence from historical observations are consistent with the detection times derived from the model projections, we use a new dataset of hourly precipitation for the

UK. It should be noted that this observational analysis uses data across the whole of the UK, whereas the model data corresponds only to the southern UK. However, we repeated the analysis with only those gauges within the model domain (Figure 1) and found this did not give any qualitative difference in the results. The provenance and extensive quality control of the observational dataset, which is comprised of ~1900 rain gauges are described in Blenkinsop et al. (2017). They indicate that although the earliest records commence in 1949, most of these gauges were installed in the 1990s and so the number for which sufficiently long records exist for trend analysis is limited. The data have been updated for this study to the end of 2014 with additional quality control procedures, including comparison with neighbouring gauges and validation against a high quality gridded daily dataset (Lewis et al., 2017). We also compared annual time series of mean 1h and 24h intensities for all gauges within 25km of each other by computing the Spearman rank (S) correlation coefficient. Such an approach ideally requires a known, reliable reference gauge to identify potential errors but in this instance most gauges correlated highly with at least one other gauge. However, one gauge (Milcote, central England) was excluded from the analysis on the basis of low correlations ($S < 0.26$ to 0.4) with three neighbouring gauges.

In addition, Blenkinsop et al. (2017) only analysed the climatology of records of ~20y length and so did not consider potential inhomogeneities that may confound any analysis of change. We therefore applied a selection of statistical tests to identify breaks in the time series that may indicate inhomogeneities in the data and in this case enabled the identification of changes in the measurement resolution of many gauges. The full details of this procedure are provided in the supporting information.

For the observational analysis we carry out several approaches to assess the change in comparison with the model projection:

i) we calculate the same three precipitation metrics as for the analysis of the model simulations for the last 13-year period of record (2002-2014) and calculate the change in each statistic relative to earlier running 13-year periods from the start of the record up to the period 1989-2001, hereafter referred to as *percentage change*;

ii) for selected 13-year periods the changes in each metric are then normalised by the variability in the metric using the same resampling procedure as for the model analysis, resampling years in the 13-year start and end periods to produce the statistic D_x. This allows a direct comparison between the observational and model analyses. We refer to this approach as *normalised change;*

iii) in addition to calculating changes in the 13-year statistics, we also calculate trends in yearly mean intensity and p_{95} values. This approach provides a less robust measure of p_{95} (since this equates to averaging only 5 hourly values in a single season assuming 5% of hours are wet, and less in the case of daily data) but allows all the observational data throughout the period of interest to contribute to the trend estimate and is an approach more typically used for the analysis of changes in a continuous time series. Trends are calculated using two methods: the longest available period at each gauge (minimum 30 years) and also using running 30-year trends calculated from 1950 at 5-year intervals (hereafter referred to as *long* and *running trends* respectively). The use of running trends allows an assessment of the sensitivity of any identified trends to the period of the record. Running trend analysis is a useful descriptive tool for climatic time series (Trottini et al., 2015) and has been used in a range of climate analyses including attribution studies (e.g.

303 Santer et al., 2014; Hamlington et al., 2013) and model evaluation (Risbey et al.,
304 2014).
305
306 For the analysis of trends, significant monotonic trends were identified using the Mann Kendall
307 test (two-tailed, 95% significance level). Trend magnitudes were estimated using the non-
308 parametric Sen's slope (Theil-Sen estimator). The Theil–Sen estimator of a set of two-
309 dimensional points (x_i,y_i) is the median of the slopes $(y_j - y_i)/(x_j - x_i)$ determined by all pairs of
310 sample points (Theil, 1950) and was extended (Sen, 1968) for cases where two data points have
311 the same *x*-coordinate (in this instance time is the *x* variable). In order to derive trends that are
312 comparable across accumulation periods we also calculated Sen's relative slope, the slope
313 joining each pair of observations being divided by the first of the pair before the overall median
314 is taken (Jassby & Cloern, 2016), providing a normalised trend that allows comparison of series
315 of different magnitudes and even units. For each period, estimated trend magnitudes for 1h
316 and 24h accumulations were also compared using a two-tailed Wilcoxon rank-sum test to test
317 for significant differences in the trend means.
318
319 Gauges were selected for this analysis of change on the basis of their completeness. For
320 assessments of the change in the 13-year statistics, gauges were only included if they were at
321 least 85% complete over the period 2002-2014 and at least one other 13-year period. For the
322 trend analysis we selected those gauges spanning at least 30 years (applying the same criteria
323 as in Blenkinsop et al. (2017) where each year/season has at least 85% of non-missing data and
324 a minimum of ~85% of years/seasons must also meet this criteria for use). Further, gauges
325 meeting these criteria were only included if missing periods did not occur at the beginning
326 and/or end of a period used for trend estimation (i.e. data present truly reflects the period for
327 which trends are estimated). In total 123(130) gauges are used in this analysis for DJF(JJA)

328 (Figure 1) but due to missing data the number available at different periods and for different
329 seasons varies, and fewer gauges were available for trend analysis due to the requirement for
330 longer, continuous time series. Sub-hourly gauge data from the UK Met Office (provided at a
331 temporal resolution of 1 min) and tipping bucket rain gauge data from the UK Environment
332 Agency were also examined but these data did not meet the record length criteria and so
333 observed change in rainfall on 10-minute timescales could not be assessed.
334
335 **c.** *Modes of variability*
336 To assess the influence of natural variability on observed trends, we examine changes in the
337 North Atlantic Oscillation (NAO) and the Atlantic Multidecadal Oscillation (AMO), using
338 the Climatic Research Unit (CRU) NAO index[1] (Jones et al., 1997) and the detrended AMO
339 index (Enfield et al., 2001) available from NOAA[2].
340
341 The NAO has long been considered the most important single mode for interpreting climate
342 variability in the northern hemisphere (Walker, 1924; Hurrell, 1996) including winter
343 precipitation in Europe (Hurrell, 1995; Hurrell & van Loon, 1997; Trigo et al., 2002; Hoy et
344 al., 2014) and has been noted to account for many of the observed changes in UK winter
345 precipitation totals and daily extremes (Simpson & Jones, 2014; Wilby et al., 1997, Brown,
346 2017). Regional variations in the association between NAO and winter rainfall have been
347 noted by Wilby et al. (2002).
348
349 Summer atmospheric circulation associated with the NAO identified by Hurrell et al. (2003)
350 has been noted to have a smaller spatial extent than in winter, and was located further north.
351 However, the summer NAO (SNAO) has been shown to have the strongest influence on

[1] Freely available at: https://crudata.uea.ac.uk/cru/data/nao/
[2] Freely available at: https://www.esrl.noaa.gov/psd/data/timeseries/AMO/

352 climate over north-western Europe (Linderholm et al., 2009; Hoy et al., 2014). Osborn et al
353 (2000) showed that ~60% of the variance in annual summer precipitation for regional series
354 for central, eastern and southern England rainfall can be explained by atmospheric circulation
355 whilst Folland et al. (2009) identified that the summer (JA) SNAO explains the principal
356 variations of summer climate over northern Europe, including mean precipitation with very
357 strong and significant negative correlations of the SNAO index with summer rainfall,
358 exceeding -0.64 over parts of the British Isles. However, Hoy et al. (2014) suggest that
359 summer relationships are sensitive to the definition of the SNAO. Simpson & Jones (2014)
360 did note some significant negative correlations between daily UK summer extreme rainfall
361 and the SNAO, and consistent with this, Brown (2017) find that positive SNAO reduces the
362 likelihood of extreme daily rainfall in summer, accounting for much of the variability from
363 1958 to 2012. In contrast, Wilby et al. (2002) identify positive correlations between the
364 SNAO and mean summer wet day amount for a cluster of sites across northern Wales and
365 England. This spatially varying response of the negative phase of the SNAO is also noted by
366 Hoy et al. (2014).
367
368 The AMO has been noted to be linked to changes in the summer NAO (Folland et al., 2009),
369 several studies suggesting that 1990s Atlantic warming was a consequence of an acceleration
370 of the Atlantic Meridional Overturning Circulation (AMOC) linked with the positive phase of
371 the winter NAO in the 1980s and 1990s (Robson et al., 2012; Lohmann et al., 2009). The
372 AMO has been identified as an indicator of the importance of the Atlantic Ocean in influencing
373 European climate, including recent wet summers in northern Europe (Sutton & Dong, 2012).
374 They indicated that coherent and consistent patterns of precipitation anomalies suggested
375 changes in atmospheric circulation associated with a warm state of the North Atlantic. We

note, however, Brown (2017) finds no influence of the AMO (as an additional covariate to the NAO) for UK daily extremes.

In the analysis here, seasonal NAO and AMO indices are calculated as the mean index value over the corresponding three months, along with 15-year moving averages for comparison with the trends in p_{95} observations.

3. Results

a. Model detection times

The convection-permitting model (CPM) simulation suggests detectable changes in 13-year mean precipitation intensity in winter may emerge across the southern UK in the 2040s (Table 2), which is in good agreement with the results of Fowler & Wilby (2010). Detection times are consistently earlier for hourly compared to daily precipitation, with differences of about 5-10 years in the median detection year across the southern UK. Detection times are also generally earlier for precipitation averaged over larger spatial scales. A similar variation in detection time is seen for changes in heavy precipitation intensity (p_{95}) in winter (Table 2). Changes in the top 1% of all values (p_{99ALL}) emerge later than changes in wet-value statistics (both mean precipitation intensity and p_{95}), with p_{99ALL} reflecting changes in both the intensity and frequency of events. The 10^{th} and 90^{th} percentiles of the spatially varying estimates of detection year (in brackets in Table 2) typically span about 40-50 years, with changes in hourly precipitation emerging in the 2030s for some local regions. Maps showing the spatial variability in detection time (Figure 2) indicate that changes in heavy precipitation may be detected earlier towards the north and west in winter, perhaps suggestive of more westerly UK winters with climate change (Malby et al., 2007).

Changes in precipitation emerge later in summer compared to winter (Table 3). For daily precipitation intensity in summer, detectable changes have not even emerged by the end of the century. However, hourly and 10-minute precipitation changes emerge earlier by many decades. For heavy 10-minute precipitation intensity, results suggest detectable changes may typically emerge across the southern UK in the 2080s. Changes in the top 1% of all values (p_{99ALL}) emerge considerably later than changes in wet-value statistics (both mean precipitation intensity and p_{95}), due to large decreases in the frequency of rainfall in summer (Chan et al., 2014a) as least partially offsetting increases in rainfall intensity for all-value statistics. There is considerable spatial variability in the detection time in summer, with the 10th and 90th percentiles of the spatial estimates (in brackets in Table 3) spanning a century or more. Maps of detection time (Figure 2) indicate there is a less clear spatial pattern in detection time in summer compared to winter. Thus in summer there is considerable uncertainty in detection time; there may be some local regions where changes in short-duration heavy summertime precipitation emerge as early as the 2050s but others where there is no detectable change well beyond the end of this century.

We note that here a constant threshold of 0.1mm has been applied to define a wet value across all accumulation periods and spatial scales. It is easier to reach a 0.1mm accumulation over a day than over a 10-minute period. In particular, since rain typically lasts longer than 10-minutes (and, in winter, longer than an hour), the daily accumulation on days with 10-minute periods exceeding 0.1mm will likely be considerably higher than 0.1mm; whilst days just exceeding the 0.1mm threshold may likely contain no individual hours or 10-minute periods selected as wet. (Note this is only the case for the model results; for the observations where there is a minimum tip ranging from 0.1mm to 0.5mm depending on gauge, detailed in the supplementary information, if a day reports 0.1mm then there must be an hour with 0.1mm.)

This then raises the question whether the finding that 10-minute precipitation changes emerge earlier is simply due to the fact we are preferentially selecting the higher intensity events at shorter accumulation periods (although there will still be considerably more 10-minute wet periods than wet days in the 13 year simulation). Looking at detection times for changes in all-value statistics (p_{99ALL}), however, shows this is not the case, with short-duration extremes consistently emerging earlier than daily extremes even when no wet-value threshold is applied. Also comparing detection times for precipitation intensity with those for heavy precipitation intensity (p_{95}) shows that detection times are not always earlier for higher intensity events (Tables 2 and 3). Thus we argue it is the impact of increasing atmospheric moisture with warming, which tends to result in rainfall falling as fewer but more intense events, that gives greater increases in intensity at shorter-accumulation periods and hence favours the earlier detection of changes in 10-minute and hourly precipitation. For the analysis of observations in the following section we focus on changes in heavy precipitation intensity (p_{95}), since these emerge earlier than all-day (and all-hour) extremes in the model. This is consistent with large decreases in rainfall occurrence (particularly in summer due to changing circulation patterns, Chan et al., 2014a) offsetting increases in rainfall intensity due to increasing atmospheric moisture. We note however that the detection time for all-day and all-hour extremes is important as this directly relates to when changes in flooding frequency will be detected (see Discussion).

Given these results are from single 13-year model realisations of the present and future climate, assume a linear trend through time, and do not account for multi-decadal natural variability (see Methods), we have low confidence in the actual detection years quoted. In particular, where detection times are beyond the end of the century, this reflects an extrapolation of the linear trend beyond the future simulation period and hence we have very low confidence in

these values especially given the projected profile of human-induced warming is far from linear over long periods. However, the finding that changes consistently emerge earlier for 10-minute compared to hourly compared to daily precipitation is expected to be more reliable. As noted above, it is consistent with the expected intensification of precipitation with climate change (Trenberth et al., 2003), such that changes in precipitation intensities are expected to be larger for shorter accumulation periods. This has been shown to be the case in summer in results from CPMs over both the UK and the Alps (Kendon et al., 2017). Results here suggest this greater signal of change dominates over any increases in noise associated with relatively greater natural variability at short timescales, at least where there is perfect sampling across space and time (but note, as discussed later, sampling issues in observational datasets may impact on this). We note variance estimates for the model control simulation agree well with observed variance for the 2002-2014 period, for both hourly and daily precipitation (Supplementary Tables S1 and S2), which gives credibility to the noise estimation that goes into the calculation of model detection time.

b. Results from observed change analysis

To examine results derived using the percentage change method we calculate the median of the percentage changes across all contributing gauges, to give a single central estimate across the UK, as well as the 10^{th} and 90^{th} percentiles of the spatially varying estimates to give an indication of uncertainty. Analysis of the results for p_{95} indicates significant spread in the magnitude of change across the gauges along with variation in the magnitude according to the periods used (Figure 3). For winter, most gauges indicate a decrease for the 2002-2014 period relative to preceding periods from those centred around 1980 onwards. In contrast, for summer, positive changes clearly emerge over the same periods, particularly for 24h accumulations. We note though that changes relative to earlier periods, particularly for summer, are characterised

by low gauge availability and so results are less robust. Similar patterns of changes are observed in the mean intensity (Figure S2) but with slightly smaller magnitude of change for summer over recent decades.

We then applied the normalised change method for three 13-year periods to more directly compare the observed changes with those from the model. The variability of each metric (obtained by resampling years in the 13-year start and end periods, see Section 2b) was used to calculate the statistic D_x where here the metric $\boldsymbol{\mu_x}$ refers to the latest 13-year period in the observations (i.e. the midpoint x is 2008) and $\boldsymbol{\mu_c}$ is the statistic for successive 13-year periods. The periods 1977-1989, 1983-1995 and 1989-2001 were selected to avoid the earlier part of the record with minimal numbers of gauges. Figure 4 shows the distribution of values of D_x for the heavy precipitation intensity metric (p_{95}). By comparison, the median D_x for the model for 100-year changes (mid year 2103 versus 2003) in p_{95} are 4.10 (2.08) for hourly precipitation at the 1.5km scale in DJF (JJA). Under the assumption that changes in p_{95} are linear through time, this would give a D_x value for the model for 25-year changes (mid-year 2028 versus 2003) of 1.03 (0.52) for hourly precipitation at the 1.5km scale in DJF (JJA). As shown in Figure 4, these model D_x values are within the 10th to 90th percentile ranges shown for the observations for a 25-year change (mid year 1983 versus 2008). Observed changes in Figure 4 are consistent with those for the percentage change in Figure 3. Winter changes in p_{95} are relatively modest and are similar for both 1h and 24h accumulations with a tendency for the period 2002-2014 to show a decrease relative to periods from the early 1980s onwards. Again, for summer, the period 2002-2014 shows potentially larger increases emerging in daily accumulations compared with hourly. The magnitude of the estimated change is sensitive to the periods used but we reiterate that longer term changes are limited by gauge availability and so may not be representative. Comparable analyses for mean intensities (Figure S3) and for p_{99ALL} (Figure

S4), along with those for p_{95} using only those gauges in the model domain (Figure S5), do not appear to present qualitatively different results and so here we focus on the analysis of heavy precipitation intensity p_{95} using pooled gauges for the whole UK to maximise the detectability of change.

We next examined the spatial pattern of the normalised change in p_{95} to explore whether any regions might emerge as potential sentinels of a climate change signal. Fowler & Wilby (2010), for example, used RCM projections to suggest that SW England could be one such region for 10 day winter precipitation totals with a 10-year return period. Here, the pattern of normalised change for hourly winter precipitation (relative to 1989-2001) is weak with some evidence of decreases tending to occur in the east (Figure S6a) whilst for summer the north and east of the UK show the strongest increases (Figure S6b). This latter pattern is replicated when compared with the period 1977-1989 but only 23 gauges are available and is also similar for daily precipitation though with a reduced regional contrast (not shown). The lack of long-term gauges means it is not possible to make robust inferences on the spatial pattern of change and so we do not consider this further in this analysis.

These results may be compared with those obtained using trends calculated using the maximum length of data available (long method) which shows that for gauges of >40 years length trends in mean winter rainfall intensity are largely positive (Figure S7a) though are not statistically significant at either the daily or hourly timescale. These positive trends are characteristic of those detected using the UK daily rain gauge network (see Section 1), however, in this analysis, over shorter, recent periods (calculated from 1980 onwards) a larger number of gauges exhibit contrasting non-significant negative trends. Comparing the mean of the relative Sen's slopes for 1h and 24h rainfall intensity (Figure S7) shows no clear pattern of a difference in trends

526 between the two timescales. This is confirmed by the absence of significant differences (95%
527 level) signified by the Wilcoxon rank-sum test. A similar pattern is seen for trends in winter
528 p_{95}, with lower positive trends and more frequent negative trends over the most recent decades
529 (Figure 5a, for relative trends, S8 and S9 for absolute trends). Using the 30y running trend
530 analysis highlights even more clearly the (multi-) decadal scale variability and trend sensitivity
531 to the period of analysis, showing a distinct shift from positive to negative trends from the
532 period 1975-2004 onwards (Figure 5b).
533
534 As noted previously, summer is characterised by a particularly low number of gauges until
535 ~1980 and so trends over earlier periods may not be representative of changes across the whole
536 of the UK, however, more gauges generally exhibit (non-significant) positive trends throughout
537 (Figure 6 for relative trends, S8-S11 for absolute trends). Another clear pattern that emerges
538 is higher relative trends at both timescales from the 1980s onwards (Figure 6a), including the
539 emergence of some trends that are statistically significant (Figures S8, S9). This is consistent
540 with the analysis using the normalised change approach and with previous work by Simpson
541 & Jones (2014) who noted that a series of wet summers starting in 2007 were beginning to
542 offset a longer term downward trend in mean and extreme UK daily summer rainfall. During
543 this later period, relative trends are also smaller for 1h than 24h accumulations, which is
544 contrary to the CPM simulation and the observed scaling of hourly and daily rainfall with
545 temperature (Chan et al., 2016a). Again, the 30y running trend analysis highlights trend
546 variability, showing an increase in the mean intensity (Figure S12) and in p_{95} (Figure 6b for
547 relative trends, S8 and S9 for absolute trends) trends for the 1985-2014 periods.
548
549 We reiterate the need for caution however in the interpretation of the temporal variability in
550 trends observed in these figures. Figures 3, 5 and 6 indicate the relatively small number of

gauges for the early period. In particular, in summer all gauges contributing records for periods from 1970 and earlier are in Scotland or Northern Ireland (Figure 1) and so may only be indicative of regional change. Only from 1980 onwards are there significant number of gauges covering England and Wales. This problem is less pronounced in winter for which the longer gauges are more evenly spatially distributed across the UK but with northern and eastern England less well represented. To explore this further we recalculated the long trends using just those gauges that provide data for all periods from 1955 onwards for consistency, thus trends for each period were based on identical gauges albeit for a very small sample (DJF:11, JJA:5). Nonetheless, there is a degree of consistency with the complete sample of gauges. In winter there is a clear decrease in the trend for 1h heavy precipitation intensity (Figure S13a) but with a less clear response of 24h totals which shows a lower sensitivity to the calculation period. Summer (JJA) is especially constrained by the limitations noted above but there is a clear tendency for increasing trends (especially for 24h) over recent decades (Figure S13b).

c. Potential contributors to trend variability

The sensitivity of observed trends to the period of calculation suggests potential influence of natural variability and so here we investigate two natural modes of variability – the North Atlantic Oscillation (NAO) and the Atlantic Multidecadal Oscillation (AMO).

Figure 7a shows the previously documented positive phases of the winter NAO in the 1980s and 1990s and subsequent decrease in the index thereafter. The positive phase of the winter NAO is associated with wetter weather in northern Europe and so trends calculated from this period are likely influenced by increased precipitation at the start of the record, potentially contributing to the lower or even decreasing trends shown in Figures 4, 5, S8 and S9. Overlaying the mean running trends of p_{95} shows consistency with the smoothed NAO time series with a marked decrease in the period after the peak of the positive NAO phase.

The notable increase in recent summer trends also corresponds with a negative phase of the summer NAO (SNAO) (Figure 7b). This is consistent with previous literature suggesting significant negative correlation of the SNAO with summer rainfall over parts of the UK (Section 2c). Figure 7c also shows a strong increase in the summer AMO since the mid-1990s, again coincident with the increase in the magnitude of running trends and percentage change for summer p_{95}. The AMO has been noted to be linked to changes in the summer NAO, as well as recent wet summers over northern Europe (Section 2c). Thus overall, the observed trends in p_{95} in summer appear to be strongly influenced by the NAO, which in turn may be related to the AMO. We also compared the teleconnection indices to variations in the ratio of the daily to hourly change in p_{95} but noted that this was relatively stable and appeared unrelated to variability in the NAO and AMO. This suggests that these modes of variability may not readily explain any differences in change between the two accumulation periods but further work might usefully investigate how natural variability affects the relative behaviour of extremes of different durations.

4. Discussion

The results here suggest it is changes in precipitation intensity (or heavy precipitation intensity) that offer the greatest promise for detecting human influence on precipitation. Such changes are linked to increasing atmospheric moisture with warming and are expected to be robust across models. Changes in precipitation extremes measured using all-values are found here to consistently emerge later, due to these reflecting changes in intensity and frequency. However, it is these changes in intensity and frequency combined which will be felt in terms of flooding. Model results here suggest that changes in summertime urban flash flooding, which respond to changes in short-duration rainfall, may not be detected this century. Changes in fluvial

601 flooding, which respond to changes in more persistent rainfall, may be detected earlier where
602 these are dominated by changes in wintertime precipitation extremes (specifically for daily
603 precipitation extremes, the CPM here suggests changes emerge in the 2060s for p_{99ALL} for
604 precipitation aggregated to the 50km scale, whilst Fowler and Wilby (2010) suggests 2040s for
605 the 10 year return level).
606
607 It is important to note that the detection time methodology has only been applied here to a
608 single realisation of future climate change from one climate model, and thus no estimate of
609 modelling uncertainty in the quoted detection times is possible. Also, it has not been possible
610 to account for the influence of multi-decadal natural variability from a single pair of 13-year
611 control and future simulations. Additional ensemble CPM experiments will allow an
612 assessment of the robustness of these results. In particular, the next set of UK climate
613 projections, to be delivered in 2018 (UKCP18), will include the first ensemble of CPM
614 simulations over the UK. This will allow a much better assessment of the influence of natural
615 climate variability, including multi-decadal variability, and hence a more robust evaluation of
616 detection time. Furthermore, coordinated multi-model ensemble experiments at convection
617 permitting scale are being carried out across Europe as part of a CORDEX Flagship Pilot Study
618 (FPS).
619
620 The results here correspond to using 13-years of data to calculate the metric for the control and
621 future periods. Using more years of data, once these become available, would make detection
622 of the change easier. In particular, where a continuous time series of data is available up to
623 2050 and beyond (as will become available with time for observations, and for CPMs is
624 planned under ongoing research at the UK Met Office beyond UKCP18), the metric could be

625 calculated for multiple (non-overlapping) periods and then detection of the change undertaken
626 using all the data. This is likely to result in earlier detection times than those quoted here.
627
628 The first major study of change in UK sub-daily rainfall observations presented here provides
629 some evidence of long-term increases in winter rainfall intensities as projected by the models.
630 In particular, these are evident in long trends for gauges with >40 years record, and are seen in
631 percentage changes between the 2002-2014 and pre-1980 periods. However, these winter
632 intensity increases are less consistent than extensive previous research on UK daily rainfall.
633 These results are however constrained here by the low number of long-term sub-daily gauges
634 available for the analysis. The observations do also exhibit the emergence of recent increases
635 in sub-daily heavy rainfall intensities in summer. However, the earlier emergence of detectable
636 changes in winter in the model is not seen in the observations, which may be explained by
637 natural variability dominating observed trends at present. Also, in contrast with the CPM
638 simulation, no consistent, significant difference between changes in 1h and 24h rainfall is
639 detected in either season. Barbero et al. (2017) similarly note an absence of the greater
640 detectability of increases in hourly extremes compared with daily for US annual and seasonal
641 maxima, except during winter. We consider that this lack of a difference between daily and
642 hourly trends compared with the CPM simulations could be due to a combination of:

643 • Relatively short records, particularly in summer, make trend detection more difficult
644 due to a low signal-to-noise ratio.
645 • A relatively sparse network of rain gauges means that we are not able to adequately
646 sample convective storms and their peak rainfall intensities on hourly timescales due to
647 the limited spatial extent of events (Agel et al., 2015; Wasko et al., 2016). By contrast,
648 winter extremes, albeit smaller in magnitude (Blenkinsop et al., 2017), are largely

649 driven by mid-latitude storms with large-scale synoptic forcing and are thus more
650 consistent in space and better captured by the sparse gauge network.

651 • Barbero et al. (2017) also hypothesize that the measurement-interval truncation
652 problem may also contribute to the lack of a trend in summer hourly extremes.
653 Maximum hourly intensities over a day are likely to be truncated due to the fixed hourly
654 intervals of precipitation measurement/recording, given that a typical convective event
655 rarely peaks exactly between two clock hours. This effect is more limited at the daily
656 timescale, as the life cycle of convective events generally does not exceed a few hours,
657 and, generally falls within a day.

658 • The signature of natural variability in terms of daily versus hourly trends may be quite
659 different from the signature of the underlying climate change signal. In particular, it
660 may only be for the latter (which is not yet emerging in the observations) where hourly
661 trends are expected to exceed daily trends.

662 The (largely non-significant) increase in summer rainfall intensities over the last three decades
663 is notable and it may seem attractive to attribute this to thermodynamic (CC related) changes.
664 However, the evidence presented here, coupled with previous research (e.g. Sutton & Dong,
665 2012) suggests that natural variability, in part related to large scale modes of variability,
666 potentially the NAO and AMO, are important drivers of extreme rainfall in the UK. This is
667 supported by Brown (2017) which showed that the NAO dominates observed trends in UK
668 summer daily rainfall extremes, in this case using a different observational dataset (the 25km
669 gridded dataset prepared for UKCP09 based on many more daily gauges). Otto et al. (2015)
670 attributed an increased risk of July 5-day rainfall extremes (but not June or August extremes)
671 for England and Wales to anthropogenic change and suggested that the AMO is not the most
672 important driver of increased precipitation. This may have been due to deficiencies in the
673 model used in their analysis or may indicate the need to investigate other possible drivers (e.g.

674 Champion et al., 2015). Similarly, the increasing number of gauges displaying negative
675 changes in winter shown by the percentage change and running trend analyses may be a
676 consequence of a weakening of the positive phase of the NAO over recent decades, including
677 a number of years when the NAO was in its negative phase towards the end of the analysis
678 period. Such modes of variability may induce long-term persistence and further contribute to
679 difficulties in identifying non-stationarity (Milly et al., 2015). Both change and trend analyses
680 over these timescales are clearly sensitive to the period of record and for precipitation, which
681 may be highly variable on decadal and multi-decadal timescales, care must be taken to consider
682 the potential drivers of this variability rather than a casual inference of a potential climate
683 change signal. A full attribution study is beyond the scope of this research but this does
684 highlight the need to consider the contribution of large-scale dynamical *and* thermodynamic
685 drivers to observed changes and natural variability in precipitation extremes. Furthermore,
686 whilst it has been proposed that adaptation planning and engineering design for infrastructure
687 be guided by the CC relationship (Zhang et al., 2017) understanding of this scaling needs to be
688 coupled with an understanding of large-scale drivers (e.g. Pfahl et al., 2017). This will not
689 only lead to improved attribution of changes but also to the improved use of models for
690 seasonal predictions and long term projections.
691
692 Notwithstanding these caveats, historical observations remain essential for a better
693 understanding of change and will aid the development of better projections of the future
694 (Montanari & Koutsoyiannis, 2014; Milly et al., 2008) and there is a particular need to develop
695 a global database for sub-daily precipitation data (Zhang et al., 2017). However, quantified
696 estimates of observed changes and trends in precipitation metrics are on their own unlikely to
697 provide sufficient understanding of, and evidence for, human-induced change for some time,
698 at least at local/regional scales across most parts of the globe for some of the reasons noted

699 above. Robustly characterising and attributing observed changes in sub-daily extremes remains
700 a considerable challenge. This is likely to be best addressed through the integrated use of high
701 quality historical observations, not only of relevant surface weather variables but also of
702 atmospheric variables, and the application of process-based models (Lenderink & Fowler,
703 2017), taking advantage of ongoing developments in convection-permitting climate modelling
704 (Prein et al., 2015), and analysis at continental scales. These challenges are currently being
705 addressed by the INTENSE (INTElligent use of climate models for adaptatioN to non-
706 Stationary hydrological Extremes) project. This project aims to establish increased synergy
707 between data, models and theory to enable the development of new downscaling approaches,
708 using information from climate models and process understanding from observations in a more
709 intelligent way. In doing so we will be better able to understand how rainfall extremes will
710 respond to a warmer world and the implications for adaptation strategies.
711

712 ## 5. Conclusion

713 Results using output from a 1.5km convection-permitting climate model over the southern UK
714 indicate that changes to 10-minute and 1h precipitation emerge before changes to daily
715 precipitation. In particular, the model results suggest detection times in the 2040s for hourly
716 rainfall intensity in winter, which are 5-10 years earlier than for daily extremes. In summer,
717 detection times are typically in the 2080s for heavy 10-minute precipitation intensity, which is
718 decades earlier than for daily extremes. However, there is considerable spatial variability in the
719 detection time, particularly in summer. These results suggest that it is changes in rainfall rates,
720 rather than changes to daily rainfall totals, which provide the greatest potential for detection of
721 change. These could manifest in increases in pluvial flooding, which predominantly affect
722 urban areas and small rapid-response catchments as flash floods. We note that it is in summer
723 when the highest hourly precipitation extremes occur in the UK (Blenkinsop et al., 2017; Chan

et al., 2014a). So even though we may be able to detect changes in precipitation extremes in winter first, the detection of changes in summer is of considerable practical value particularly for the management of urban flash flooding. Hence the considerably earlier emergence of short-duration extremes compared to daily extremes in summer is important.

Results from a new quality-controlled dataset of hourly rainfall over the UK do not show a similar difference between daily and hourly changes. This appears to be explained by natural variability dominating trends in current observational records, although as warming strengthens the climate change signal may become more apparent. In general, the relative changes at hourly versus daily timescales may be a useful signature of underlying climate change that could be employed in detection and attribution studies. Although results presented here are for the UK, this signature is expected to apply more widely. In particular, where increasing atmospheric moisture with warming is the dominant driver of precipitation change, we may expect precipitation rates to intensify and the earlier emergence of detectable changes in short-duration precipitation intensities. There are also local feedbacks within storms, linked to latent heat release, which have been proposed to explain greater increases in rainfall extremes on hourly timescales (Lenderink & van Meijgaard, 2010; Lenderink et al., 2017) and are expected to apply more generally in convective regimes and seasons. This is consistent with the model results here showing that it is in summer, in particular, when hourly and sub-hourly extremes emerge much sooner than daily ones, as this is the season when convective storms are more prevalent.

Providing robust quantitative estimates of when we may be able to detect the influence of climate change on rainfall extremes is important for informing adaptation planning. The results presented here are from a single realisation of future climate change from one climate model,

and so we have low confidence in the actual detection years quoted. Providing robust estimates of detection time will require additional CPM ensemble experiments that are currently planned over the UK as part of the UKCP18 project and more widely as part of coordinated multi-model projects (e.g. CORDEX-FPS).

Current guidance on climate change allowances for rainfall for the purposes of UK flood risk management is provided by Defra (Defra, 2006) and the Environment Agency (Environment Agency, 2011), and specifies peak rainfall intensity increases of 5% (1990-2025), 10% (2025-2055), 20% (2055-2085) and 30% (2085-2115) relative to a 1961-90 baseline. However this guidance is not designed to be applied to sub-daily rainfall (the need for revised guidance is noted in Dale et. al., 2017). Results here suggest separate climate change allowances need to be developed for hourly and sub-hourly rainfall, the latter being particularly important for urban flash flooding. Such allowances will need to be specified for changes emerging over the next few decades. Thus future work will focus on exploiting the first ensemble of climate simulations at convection-permitting scale from UKCP18 to provide robust estimates of change in sub-daily rainfall extremes to inform updated national guidance on climate change allowances.

6. Acknowledgements

E.J. Kendon gratefully acknowledges funding from the Joint Department of Energy and Climate Change (DECC) and Department for Environment Food and Rural Affairs (Defra) Met Office Hadley Centre Climate Programme (GA01101). This work also forms part of a joint UK Met Office and Natural Environment Research Council (UKMO-NERC) funded project on Convective Extremes (CONVEX, NE/1006680/1) and the European Research Council funded INTENSE project (ERC-2013-CoG-617329). H.J. Fowler is also funded by the Wolfson

774 Foundation and the Royal Society as a Royal Society Wolfson Research Merit Award
775 (WM140025) holder. We would like to thank Dr Renaud Barbero for conducting the
776 assessment of the statistical tests for break points and Dr Steven Chan for contributing to the
777 running of the climate model simulations.

References

Agel, L., Barlow M, Qian JH, Colby F, Douglas E, Eichler T, 2015. Climatology of daily precipitation and extreme precipitation events in the northeast United States, *J. Hydrometeorol.*, **16(6)**, 2537–2557.

Allen MR, Ingram WJ, 2002, "Constraints on future changes in climate and the hydrologic cycle" *Nature* **419** 224-232.

Archer DR, Fowler HJ, 2015. Characterising flash flood response to intense rainfall and impacts using historical information and gauged data in Britain. *J. Flood Risk Manage.* doi:10.1111/jfr3.12187.

Arnbjerg-Nielsen K, Willems P, Olsson J, Beecham S, Pathirana A, Bülow Gregersen I, Madsen H, Nguyen V T V, 2013. Impacts of climate change on rainfall extremes and urban drainage systems: a review. *Water Science and Technology* **68** 16-28.

Barbero R, Fowler HJ, Lenderink G, Blenkinsop S. 2017. Is the intensification of precipitation extremes with global warming better detected at hourly than daily resolutions?, Geophys. Res. Lett., 43, doi:10.1002/2016GL071917.

Berg P, Moseley C, Haerter JO, 2013. Strong increase in convective precipitation in response to higher temperatures. *Nature Geosci.* 6, 181-185.

Blenkinsop S, Chan SC, Kendon EJ, Roberts NM, Fowler HJ, 2015. Temperature influences on intense UK hourly precipitation and dependency on largescale circulation. *Environ. Res. Lett.*, 10, 054021.

Blenkinsop S, Lewis E, Chan SC, Fowler HJ, 2017. An hourly precipitation dataset and climatology of extremes for the UK. *International Journal of Climatology*, **37**, 722–740.

Brown S, 2017. The drivers of variability in UK extreme rainfall. *International Journal of Climatology*, doi:10.1002/joc.5356.

Cabinet Office & DEFRA, 2016. National Flood Resilience Review, HM Government, pp145.

Champion AJ, Allan RP, Lavers DA, 2015. Atmospheric rivers do not explain UK summer extreme rainfall. *J. Geophys. Res. Atmos.*, **120**, 6731–6741.

Chan, S. C., E. J. Kendon, H. J. Fowler, S. Blenkinsop, C. A. T. Ferro, and D. B. Stephenson, 2013. Does increasing the spatial resolution of a regional climate model improve the simulated daily precipitation? *Climate Dyn*., 41, 1475–1495, doi:10.1007/s00382-012-1568-9.

Chan, S. C., E. J. Kendon, H. J. Fowler, S. Blenkinsop, and N. M. Roberts, 2014a: Projected increases in summer and winter UK sub-daily precipitation extremes from high resolution regional climate models. *Environ. Res. Lett*., 9, 084 019, doi:10.1088/1748-9326/9/8/084019.

Chan S.C., Kendon E.J., Fowler H.J., Blenkinsop S., Roberts N., Ferro C.A.T., 2014b. The value of high-resolution Met Office regional climate models in the simulation of multi-hourly precipitation extremes. *Journal of Climate*, **27**, 6155-6174.

Chan SC, Kendon EJ, Roberts NM, Fowler HJ, Blenkinsop S. 2016a. Downturn in scaling of UK extreme rainfall with temperature for future hottest days. *Nature Geosci.*, 9**,** 24-28.

Chan SC, Kendon EJ, Roberts NM, Fowler HJ, Blenkinsop S, 2016b. The characteristics of summer sub-hourly rainfall over the southern UK in a high-resolution convective permitting model. *Env. Res. Lett.*, **11**, 094024.

Dale, M., B. Luck, H.J. Fowler, S. Blenkinsop, E. Gill, J. Bennett, E.J. Kendon, S.C. Chan, 2017. New climate change rainfall estimates for sustainable drainage, 170 (4)

(August 2017; themed issue on sustainable adaptation - part 1) Engineering Sustainability, doi:10.1680/jensu.15.00030

Darch GJC, McSweeney RT, Kilsby CG, Jones PG, Osborn TJ, Tomlinson JE, 2016. Analysing changes in short-duration extreme rainfall events. Proceedings of the Institution of Civil Engineers - Water Management, **169**, 201-211

Defra, 2006. Flood and Coastal Defence Appraisal Guidance FCDPAG3 Economic Appraisal – Supplementary note to operating authorities – climate change impacts, s.I.: Defra

Enfield, D.B., A.M. Mestas-Nunez, and P.J. Trimble, 2001: The Atlantic Multidecadal Oscillation and its relationship to rainfall and river flows in the continental U.S., *Geophys. Res. Lett.*, **28**, 2077-2080.

Environment Agency, 2011. Adapting to climate change: advice for flood and coastal erosion risk management authorities, Environment Agency.

Faulkner, D.S., 1999. Rainfall frequency estimation. Volume 2 of the *Flood Estimation Handbook*. Centre for Ecology & Hydrology.

Fischer EM, Knutti R, 2016. Observed heavy precipitation increase confirms theory and early models. *Nature Clim. Change*, **6,** 986-991.

Folland, CK, Knight J , Linderholm HW, Fereday D, Ineson S, Hurrell JW, 2009. The Summer North Atlantic Oscillation: Past, Present, and Future. *J. Climate*, **22**, 1082–1103,

Fowler HJ, Kilsby CG. 2003a. A regional frequency analysis of United Kingdom extreme rainfall from 1961 to 2000. *International Journal of Climatology* **23:** 1313-1334.

Fowler HJ, Kilsby CG. 2003b. Implications of changes in seasonal and annual extreme rainfall. *Geophysical Research Letters* **30**: 1720.

852 Fowler HJ, Cooley D, Sain SR, Thurston M, 2010. Detecting change in UK extreme
853 precipitation using results from the climateprediction.net BBC Climate Change
854 Experiment. *Extremes*, **13(2),** 241-267, doi:10.1007/s10687-010-0101-y.
855 Fowler HJ**,** Wilby RL, 2010. Detecting changes in seasonal precipitation extremes using
856 regional climate model projections: Implications for managing fluvial flood
857 risk. *Water Resources Research,* **46,** W03525.
858 Hamlington BD, Leben RR, Strassburg MW, Nerem RS, Kim K.-Y., 2013. Contribution of the
859 Pacific Decadal Oscillation to global mean sea level trends, *Geophys. Res.*
860 *Lett.*, **40**, 5171–5175, *doi:*10.1002/grl.50950.
861 Hegerl GC, Black E, Allan RP, Ingram WJ, Polson D, Trenberth KE, Chadwick RS, Arkin PA,
862 Sarojini BB, Becker A, Dai A, Durack PJ, Easterling D, Fowler HJ, Kendon
863 EJ, Huffman GJ, Liu C, Marsh R, New M, Osborn TJ, Skliris N, Stott PA,
864 Vidale PL, Wijffels SE, Wilcox LJ, Willett KM, Zhang X. 2015. Challenges
865 in Quantifying Changes in the Global Water Cycle. *Bull. Amer. Meteor. Soc.*,
866 **96**: 1097–1115, doi: 10.1175/BAMS-D-13-00212.1.
867 Hoy, A., Schucknecht, A., Sepp, M., Matschullat J, 2014. Large-scale synoptic types and
868 their impact on European precipitation. *Theor Appl Climatol*, **116**, 19-35.
869 Hurrell, JW, 1995. Decadal Trends in the North Atlantic Oscillation: Regional Temperatures
870 and Precipitation. *Science*, **269,** 676-679.
871 Hurrell, JW, 1996. Influence of variations in extratropical wintertime teleconnections on
872 northern hemisphere temperature. *Geophysical Research Letters*, **23,** 665-668.
873 Hurrell JW, Kushnir Y, Ottersen G, Visbeck M. 2003. An overview of the North Atlantic
874 Oscillation. The North Atlantic Oscillation: climatic significance and
875 environmental impact. *Geophysical Monograph*, **134**, 1–35.

876 Jassby AD, Cloern JE, 2016. wq: Some tools for exploring water quality monitoring data. R
877 package version 0.4.7. http://cran.r-project.org/package=wq.
878 Jenkins GJ, Perry MC, Prior MJ. 2008. *The climate of the United Kingdom and recent trends*.
879 Met Office Hadley Centre, Exeter, UK.
880 Jones MR, Fowler HJ, Kilsby CG, Blenkinsop S. 2013. An assessment of changes in seasonal
881 and annual extreme rainfall in the UK between 1961 and 2009. *International*
882 *Journal of Climatology* **33**: 1178–1194.
883 Jones, P.D., Jónsson, T. and Wheeler, D., 1997: Extension to the North Atlantic Oscillation
884 using early instrumental pressure observations from Gibraltar and South-West
885 Iceland. *Int. J. Climatol.*, **17**, 1433-1450.
886 Kendon E.J., Roberts N.M., Senior C.A., Roberts M.J., 2012. Realism of rainfall in a very high
887 resolution regional climate model. *Journal of Climate,* **25**, 5791-5806.
888 Kendon EJ, Roberts NM, Fowler HJ, Roberts MJ, Chan SC, Senior CA, 2014. Heavier summer
889 downpours with climate change revealed by weather forecast resolution model.
890 *Nature Clim. Change*, **4**, 570–576.
891 Kendon EJ, Ban N, Roberts NM, Fowler HJ, Roberts MJ, Chan SC, Evans JP, Fosser G,
892 Wilkinson JM, 2017. Do convection-permitting regional climate models
893 improve projections of future precipitation change? *BAMS.*, **98** (1), 79-, doi:
894 10.1175/BAMS-D-15-0004.1.
895 Lean, H.W., P.A. Clark, M. Dixon, N.M. Roberts, A. Fitch, R. Forbes, and C. Halliwell,
896 2008. Characteristics of high-resolution versions of the Met Office Unified
897 Model for forecasting convection over the United Kingdom, *Mon. Weather*
898 *Rev*., 136, 3408--3424, doi:10.1175/2008MWR2332.1
899 Lenderink G, Fowler HJ, 2017. Hydroclimate: Understanding Precipitation Extremes. *Nature*
900 *Climate Change,* doi:10.1038/nclimate3305.

Lenderink G, van Meijgaard E. 2008. Increase in hourly precipitation extremes beyond expectations from temperature changes, *Nat. Geosci.*, **1**, 511–514.

Lenderink G, van Meijgaard E. 2010. Linking increases in hourly precipitation extremes to atmospheric temperature and moisture changes, *Environ. Res. Lett.*, **5(2)**, 025,208.

Lenderink, G., Barbero, R., Loriaux, J.M., Fowler, H.J. 2017. Super Clausius-Clapeyron scaling of extreme hourly precipitation and its relation to large-scale atmospheric conditions. *Journal of Climate*, DOI: 10.1175/JCLI-D-16-0808.1

Lewis E, Quinn N, Blenkinsop S, Freer J, Fowler HJ, Coxon, Bates, Woods, 2017. A gridded hourly precipitation dataset for the UK. Submitted, *Journal of Hydrology*.

Linderholm, H. W., Folland, C. K. and Walther, A. (2009), A multicentury perspective on the summer North Atlantic Oscillation (SNAO) and drought in the eastern Atlantic Region. *J. Quaternary Sci.*, **24**, 415–425.

Lohmann K, Drange H, Bentsen M, 2009. Response of the North Atlantic subpolar gyre to persistent North Atlantic oscillation like forcing. Climate Dynamics, **32**, 273-285.

Loriaux JM, Lenderink G, De Roode SR, Siebesma AP, 2013. Understanding Convective Extreme Precipitation Scaling Using Observations and an Entraining Plume Model. *Journal of the Atmospheric Sciences*, **70,** 3641-3655.

Malby AR, Whyatt JD, Timmis RJ, Wilby RL, Orr HG, 2007. Long-term variations in orographic rainfall: analysis and implications for upland catchments. *Hydrological Sciences Journal*, 52(2):276-91.

Maraun D, Osborn TJ, Gillett NP. 2008. United Kingdom daily precipitation intensity: improved early data, error estimates and an update from 2000 to 2006. *International Journal of Climatology* **28**: 833-842.

926 Milly PCD, Betancourt J, Falkenmark M, Hirsch RM, Kundzewicz ZW, Lettenmaier DP,
927 Stouffer RJ, 2008. Stationarity Is Dead: Whither Water Management? *Science*,
928 **319**, 573-574. doi: 10.1126/science.1151915.
929 Milly PCD, Betancourt J, Falkenmark M, Hirsch RM, Kundzewicz ZW, Lettenmaier DP,
930 Stouffer RJ, Dettinger MD, Krysanova V, 2015. On Critiques of "Stationarity
931 is Dead: Whither Water Management?" *Water Resources Research*, **51**, 7785-
932 7789. doi:10.1002/2015WR017408.
933 Min S-K, Zhang X, Zwiers F W, Hegerl G C, 2011. Human contribution to more-intense
934 precipitation extremes. *Nature* **470** 378-381.
935 Mishra V, Wallace JM, Lettenmaier DP, 2012. Relationship between hourly extreme
936 precipitation and local air temperature in the United States, *Geophys. Res. Lett.*,
937 **39**, L16403.
938 Montanari A, Koutsoyiannis D, 2014. Modeling and mitigating natural hazards: Stationarity is
939 immortal!" *Water Resources Research*, **50**, 9748-9756.
940 doi:10.1002/2014WR016092.
941 Murphy JM, Sexton DMH, Jenkins GJ, Boorman PM, Booth BBB, Brown CC, Clark RT,
942 Collins, M., Harris GR, Kendon EJ, Betts RA, Brown SJ, Howard TP,
943 Humphrey KA, McCarthy MP, McDonald RE, Stephens A, Wallace C, Warren
944 R, Wilby R, Wood RA, 2009. *UK Climate Projections Science Report: Climate*
945 *change projections*. Met Office Hadley Centre, Exeter.
946 Osborn TJ, Hulme M. 2002. Evidence for trends in heavy rainfall events over the UK.
947 *Philosophical Transactions of the Royal Society of London. Series A:*
948 *Mathematical, Physical and Engineering Sciences* **360**: 1313-1325.

949 Osborn TJ, Hulme M, Jones PD, Basnett TA. 2000. Observed trends in the daily intensity of
950 United Kingdom precipitation. *International Journal of Climatology* **20**: 347-
951 364.
952 Otto FEL, Rosier SM, Allen MR, Massey NR, Rye CJ, Quintana JI, 2015. Attribution analysis
953 of high precipitation events in summer in England and Wales over the last
954 decade. *Climatic Change,* **132** 77-91.
955 Pall P, Allen M R, Stone D A, 2007, "Testing the Clausius–Clapeyron constraint on changes
956 in extreme precipitation under CO2 warming" *Climate Dynamics* **28** 351-363.
957 Pall P, Aina T, Stone D A, Stott P A, Nozawa T, Hilberts A G J, Lohmann D, Allen M R,
958 2011, Anthropogenic greenhouse gas contribution to flood risk in England
959 and Wales in autumn 2000. *Nature* **470** 382-385. doi:10.1038/nature09762.
960 Pfahl S, Ogorman PA, Fischer EM, 2017. Understanding the regional pattern of projected
961 future changes in extreme precipitation. *Nature Clim. Change*,
962 doi:10.1038/nclimate3287.
963 Prein AF, Langhans W, Fosser G, Ferrone A, Ban N, Goergen K, Keller M, Tölle M, Gutjahr
964 O, Feser F, Brisson E, Kollet S, Schmidli J, van Lipzig NPM, Leung R, 2015. A
965 review on regional convection-permitting climate modeling: Demonstrations,
966 prospects, and challenges, *Rev. Geophys.*, **53**, 323–361.
967 Risbey JS, Lewandowsky S, Langlais C, Monselesan DP, O'Kane TJ, Oreskes N, 2014. Well-
968 estimated global surface warming in climate projections selected for ENSO
969 phase. *Nature Clim. Change*, **4**, 835-840. doi:10.1038/nclimate2310.
970 Robson J, Sutton R, Lohmann K, Smith D, Palmer MD, 2012: Causes of the Rapid Warming
971 of the North Atlantic Ocean in the Mid-1990s. *J. Climate*, **25**, 4116–4134.
972 Santer BD, Bonfils C, Painter JF, Zelinka MD, Mears C, Solomon S, Schmidt GA, Fyfe JC,
973 Cole JN S, Nazarenko L, Taylor KE, Wentz FJ, 2014. Volcanic contribution

974 to decadal changes in tropospheric temperature. *Nature Geosci.* **7** 185-189.
975 doi:10.1038/ngeo2098.
976 Sarojini BB, Stott PA, Black E. 2016. Detection and attribution of human influence on regional
977 precipitation. Nature Climate Change **6:** 669-675.
978 Schaller N, Kay A L, Lamb R, Massey N R, van Oldenborgh G J, Otto F E L, Sparrow S N,
979 Vautard R, Yiou P, Ashpole I, Bowery A, Crooks S M, Haustein K,
980 Huntingford C, Ingram W J, Jones R G, Legg T, Miller J, Skeggs J, Wallom D,
981 Weisheimer A, Wilson S, Stott P A, Allen M R, 2016. Human influence on
982 climate in the 2014 southern England winter floods and their impacts. *Nature*
983 *Clim. Change*, **6**, 627-634.
984 Sen PK, 1968. Estimates of the regression coefficient based on Kendall's tau. Journal of the
985 American Statistical Association, 63, 1379–1389, doi:10.2307/2285891.
986 Simpson IR, Jones PD, 2014. Analysis of UK precipitation extremes derived from Met Office
987 gridded data. *International Journal of Climatology* **34**: 2438–2449.
988 Stein THM, Hogan RJ, Clark PA, Halliwell CE, Hanley KE, Lean HW, Nicol JC and Plant RS,
989 2015. The DYMECS Project: A Statistical Approach for the Evaluation of
990 Convective Storms in High-Resolution NWP Models, *Bull. Am. Meteorol. Soc*.
991 939–951
992 Sutton RT, Dong B, 2012. Atlantic Ocean influence on a shift in European climate in the 1990s.
993 *Nature Geosci*., **5**, 788-792.
994 Theil H, 1950. A rank-invariant method of linear and polynomial regression analysis. *I. Proc.*
995 *Kon. Ned. Akad. v. Wetensch*. *Ser A53*, 386-392 (Part I), 521-525 (Part II),
996 1397-1412 (Part III).
997 Trenberth KE, Dai A, Rasmussen RM, Parsons DB, 2003. The changing character of
998 precipitation. *Bull. Amer. Meteor. Soc.*, **84**, 1205–1217.

Trigo RM, Osborn TJ, Corte-Real J, 2002. The North Atlantic Oscillation influence on Europe: climate impacts and associated physical mechanisms. *Climate Research,* **20,** 9-17.

Trottini M, Isabel M, Aguiar V, Palazón SB, 2015: On the Use of Running Trends as Summary Statistics for Univariate Time Series and Time Series Association. *J. Climate,* **28**, 7489–7502, doi: 10.1175/JCLI-D-15-0009.1.

Walker GT (1924) Correlations in seasonal variations of weather. IX Mem Ind Meteorol Dept, **24**:275–332.

Walters, D.N., M.J. Best, A.C. Bushell, D. Copsey, J.M. Edwards, P.D. Falloon, C.M. Harris, A.P. Lock, J.C. Manners, C.J. Morcrette, M.J. Roberts, R.A. Stratton, S. Webster, J.M. Wilkinson, M.R. Willett, I.A. Boutle, P.D. Earnshaw, P.G. Hill, C.MacLachlan, G.M. Martin, W. Moufouma-Okia, M.D. Palmer, J.C. Petch, G.G. Rooney, A.A. Scaife, and K.D. Williams, 2011. The Met Office Unified Model global atmosphere 3.0/3.1 and JULES global land 3.0/3.1 configurations. *Geosci. Model Devel*., 4, 919--941, doi:10.5194/gmd-4-919-2011.

Wasko, C., Sharma A, Westra S, 2016. Reduced spatial extent of extreme storms at higher temperatures, *Geophys. Res. Lett.*, **43**, 4026–4032.

Westra S, Fowler HJ, Evans JP, Alexander LV, Berg P, Johnson F, Kendon EJ, Lenderink G, Roberts NM, 2014. Future changes to the intensity and frequency of short-duration extreme rainfall, *Rev. Geophys.*, 52,522–555, doi:10.1002/2014RG000464.

Westra S, Sisson SA, 2011. Detection of non-stationarity in precipitation extremes using a max-stable process model. *Journal of Hydrology,* **406,** 119-128. doi:10.1016/j.jhydrol.2011.06.014.

Wilby, R. L., O'Hare, G. and Barnsley, N., 1997. The North Atlantic Oscillation and British Isles climate variability, 1865–1996. *Weather*, **52**, 266–276.

Wilby RL, Conway D, Jones PD, 2002. Prospects for downscaling seasonal precipitation variability using conditioned weather generator parameters. *Hydrol. Process.*, **16**, 1215–1234.

Zhang X, Zwiers FW, Li G, Wan H, Cannon AJ, 2017. Complexity in estimating past and future extreme short-duration rainfall. *Nature Geoscience*, **10**, 255–259. doi:10.1038/ngeo2911.

Period	DJF	JJA
Percentage/normalised change	108	115
Long trends	63	72
Running trends	73	78
Combined unique	123	130

Table 1: Number of gauges available for each season and for each method used for the analysis of change. The total number of unique gauges is also shown.

	1.5km	5km	12km	50km
Precipitation intensity				
daily	2050 (2033, 2086)	2051 (2033, 2090)	2051 (2034, 2092)	2050 (2033, 2100)
hrly	2048 (2034, 2071)	2046 (2034, 2073)	2045 (2034, 2075)	2041 (2032, 2060)
Heavy precipitation intensity p_{95}				
daily	2056 (2042, 2084)	2056 (2042, 2085)	2055 (2041, 2084)	2054 (2040, 2077)
hrly	2051 (2032, 2073)	2050 (2032, 2072)	2048 (2032, 2069)	2042 (2032, 2061)
Heavy precipitation p_{99ALL}				
daily	2071 (2048, 2117)	2070 (2048,2115)	2069 (2048,2112)	2061 (2044,2098)
hrly	2055 (2033,2084)	2055 (2033,2082)	2053 (2034,2078)	2050 (2034,2071)

Table 2: Median detection year across southern UK land points for changes in (top) precipitation intensity, (middle) heavy precipitation intensity p_{95} and (bottom) heavy precipitation p_{99ALL} in winter, for precipitation accumulated across a range of space (1.5km-50km) and time (hrly-daily) scales. Also shown in brackets are the 10th and 90th percentiles of the spatially varying estimates of detection year. Precipitation intensity is defined as the mean of wet values (>0.1mm per accumulation period) over the 13-year period, heavy precipitation intensity is defined as the mean of the upper 5% of wet values (p_{95}), and heavy precipitation is defined as the mean of the upper 1% of all values (p_{99ALL}).

	1.5km	5km	12km	50km
Precipitation intensity				
daily	2252 (2117, 3211)	2261 (2119, 3247)	2261 (2124, 3426)	2325 (2129, 4195)
hrly	2123 (2078, 2299)	2121 (2076, 2315)	2116 (2072, 2289)	2121 (2079, 2314)
10min	2107 (2072, 2198)	2100 (2068, 2186)	2093 (2062, 2171)	2114 (2069, 2187)
Heavy precipitation intensity p_{95}				
daily	2178 (2095, 2814)	2186 (2099, 2858)	2210 (2107, 3027)	2266 (2138, 2874)
hrly	2097 (2064, 2182)	2095 (2062, 2179)	2096 (2062, 2188)	2126 (2085, 2257)
10min	2088 (2059, 2157)	2083 (2054, 2146)	2091 (2056, 2179)	2184 (2084, 2543)
Heavy precipitation p_{99ALL}				
daily	2308 (2126,3625)	2320 (2128,3617)	2314 (2131,3514)	2329 (2127,3006)
hrly	2175 (2092,2744)	2188 (2097,2821)	2205 (2105,2974)	2211 (2124,5058)
10min	2107 (2069,2224)	2119 (2075,2273)	2147 (2088,2454)	2211 (2121,3572)

Table 3: As Table 2, but for changes in (top) precipitation intensity, (middle) heavy precipitation intensity p_{95} and (bottom) heavy precipitation p_{99ALL} in summer. In this season, results are also available for 10-minute precipitation.

Figure caption list

Figure 1: Sub-daily rain gauges included in the analyses for a) DJF (123 gauges), and b) JJA (130 gauges). Years denote the first year in the earliest 13y analysis period meeting the required level of completeness. Line denotes northern limit of the CPM simulation domain.

Figure 2: Spatial variation in detection year across the southern UK for changes in heavy precipitation intensity p_{95} in (left) winter and (right) summer, for hourly precipitation at 5km scale. Heavy precipitation intensity is defined as the mean of the upper 5% of wet values (p_{95}).

Figure 3: Percentage change in heavy rainfall intensity (Δp_{95}) for the period 2002-2014 relative to successive rolling 13-year periods in the observations (top row 1h, middle row 24h). Change is plotted at the midpoint of the earlier 13-year period. The solid line denotes the median of the change across all available gauges, the shading denotes the range bounded by the 10^{th} and 90^{th} percentile ranges where at least 15 gauges are available. The horizontal lines indicate the periods used to resample the observed time series to evaluate normalised change. The bar plots (bottom row) denote the number of gauges available for each period.

Figure 4: Distribution of normalised change in heavy rainfall intensity (p_{95}, D_x) for 1h and 24h accumulations for the period 2002-2014 relative to three 13 year periods in the observations. The black triangles denote the median of the corresponding 1.5km model results for a 25-year change (scaled linearly from the 100-year change). The value *n* denotes the number of gauges available for each period used to calculate change.

Figure 5: Relative Sen's slope (unitless) for winter (DJF) hourly and daily heavy rainfall intensity (p_{95}) in the observations for a) successive periods ending in 2014 (long

trends) and b) successive 30y periods (running trends). Points show mean slope of all gauges whilst ranges show the 95% confidence interval estimated using the Student's t distribution when the number of gauges n >=15 (see Supporting Information for method details). Lower plots shows the number of gauges used for each period.

Figure 6: As in Figure 5 but for summer (JJA) hourly and daily heavy rainfall intensity (p_{95}) in the observations.

Figure 7: Time series of teleconnection indices for a) DJF NAO, b) JJA NAO, c) JJA AMO. The black line denotes the 15-year moving average. The orange and green lines indicate the mean seasonal relative Sen's slope for 1h and 24h p_{95} using running trends for each 30-year period plotted at the mid-year.

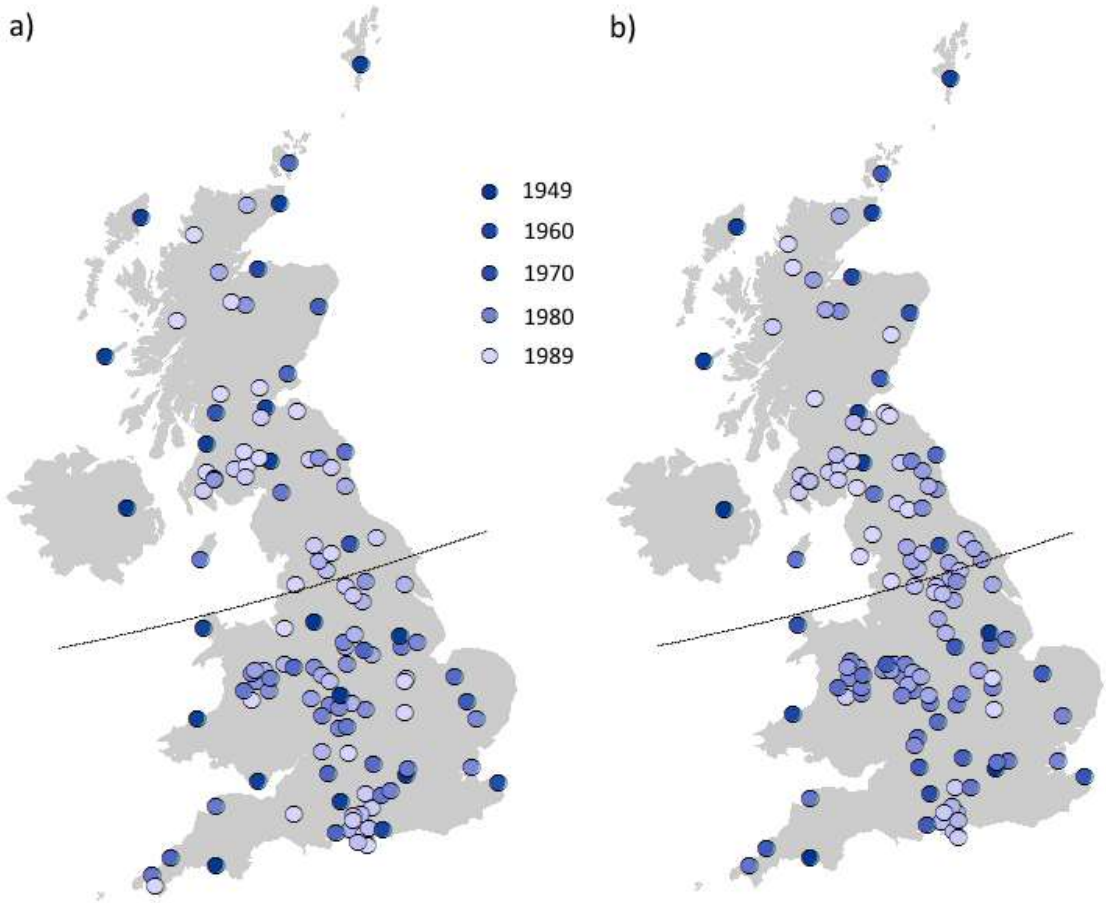

Figure 1: Sub-daily rain gauges included in the analyses for a) DJF (123 gauges), and b) JJA (130 gauges). Years denote the first year in the earliest 13y analysis period meeting the required level of completeness. Line denotes northern limit of the CPM simulation domain.

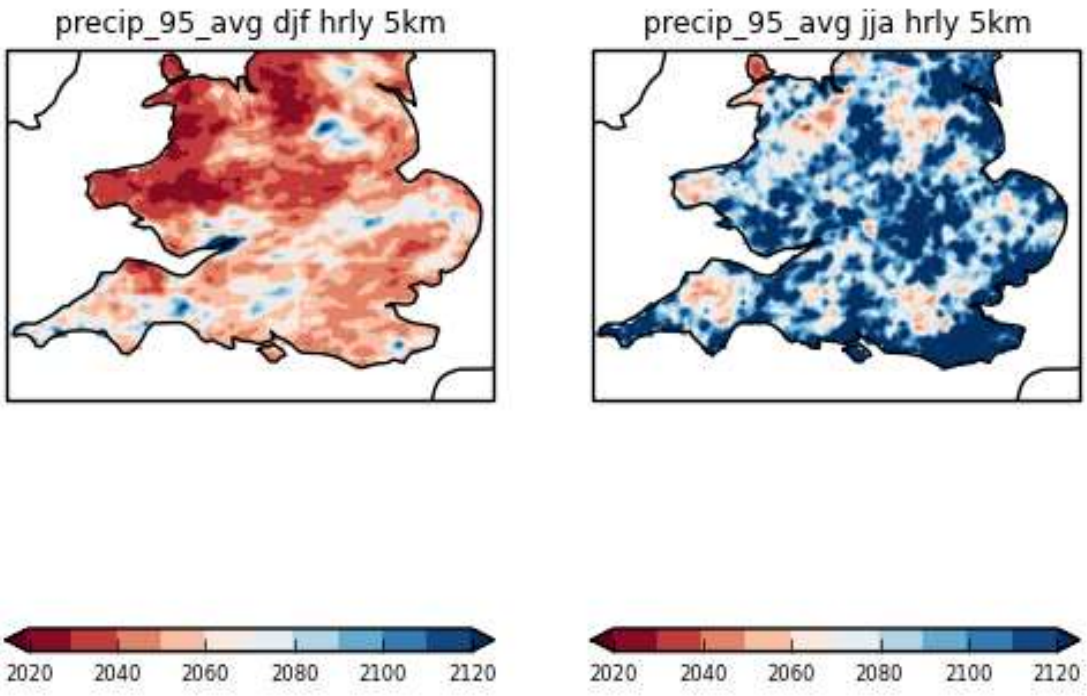

Figure 2: Spatial variation in detection year across the southern UK for changes in heavy precipitation intensity p_{95} in (left) winter and (right) summer, for hourly precipitation at 5km scale. Heavy precipitation intensity is defined as the mean of the upper 5% of wet values (p_{95}).

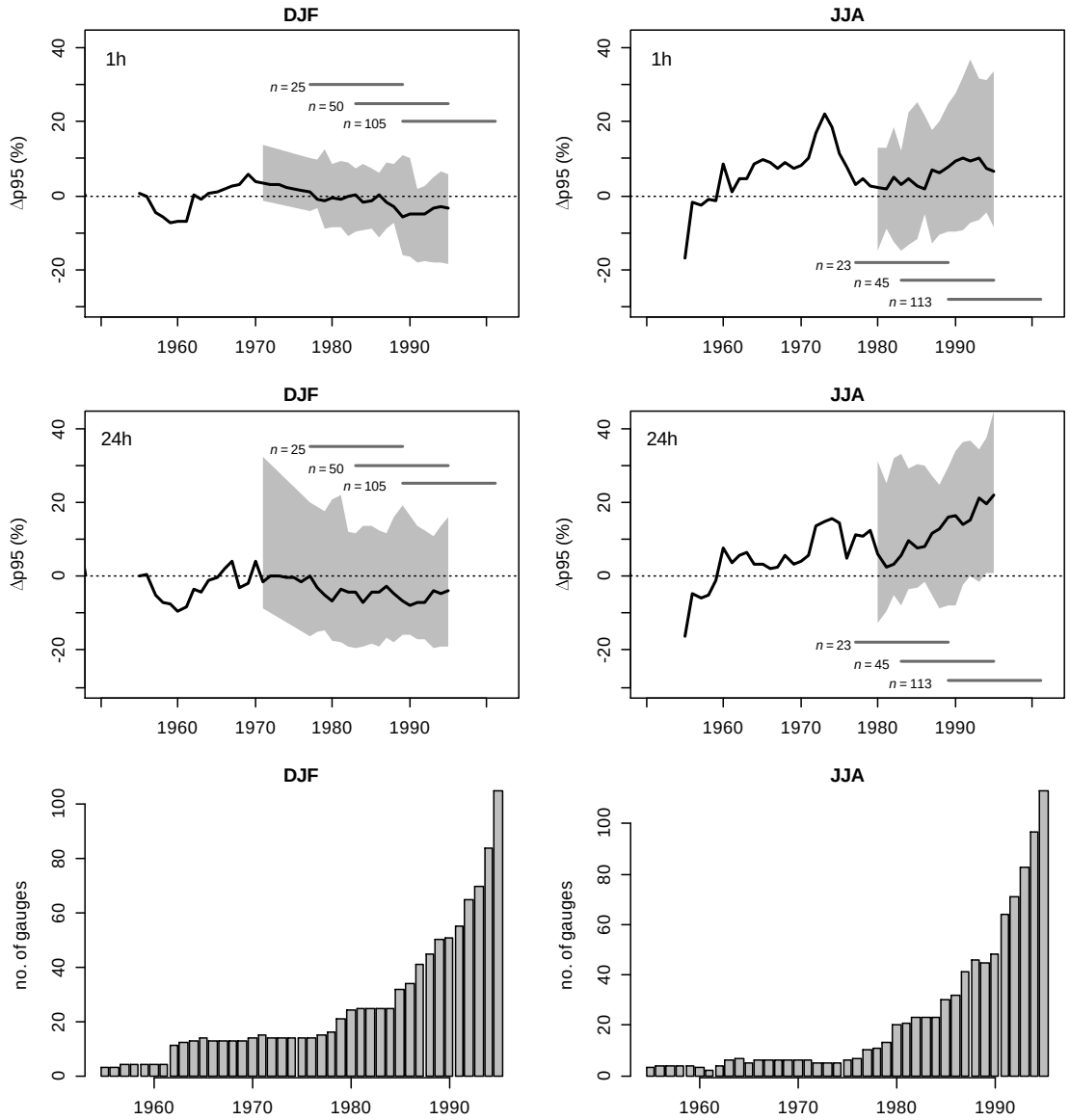

Figure 3: Percentage change in heavy rainfall intensity (Δp_{95}) for the period 2002-2014 relative to successive rolling 13-year periods in the observations (top row 1h, middle row 24h). Change is plotted at the midpoint of the earlier 13-year period. The solid line denotes the median of the change across all available gauges, the shading denotes the range bounded by the 10th and 90th percentile ranges where at least 15 gauges are available. The horizontal lines indicate the periods used to resample the observed time series to evaluate normalised change. The bar plots (bottom row) denote the number of gauges available for each period.

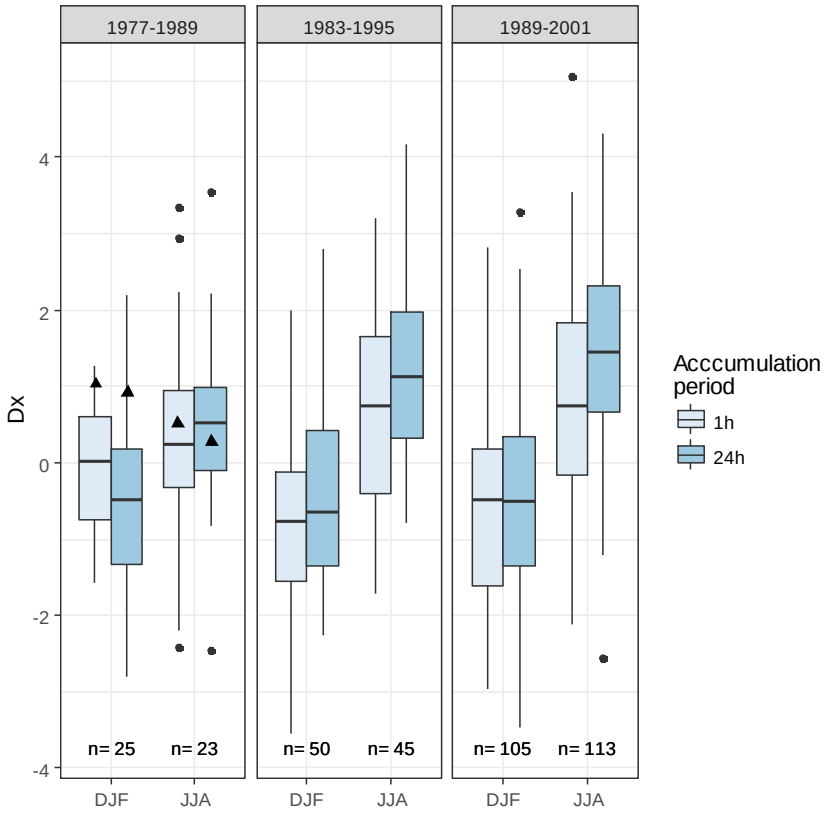

Figure 4: Distribution of normalised change in heavy rainfall intensity ($p_{95,} D_x$) for 1h and 24h accumulations for the period 2002-2014 relative to three 13 year periods in the observations. The black triangles denote the median of the corresponding 1.5km model results for a 25-year change (scaled linearly from the 100-year change). The value *n* denotes the number of gauges available for each period used to calculate change.

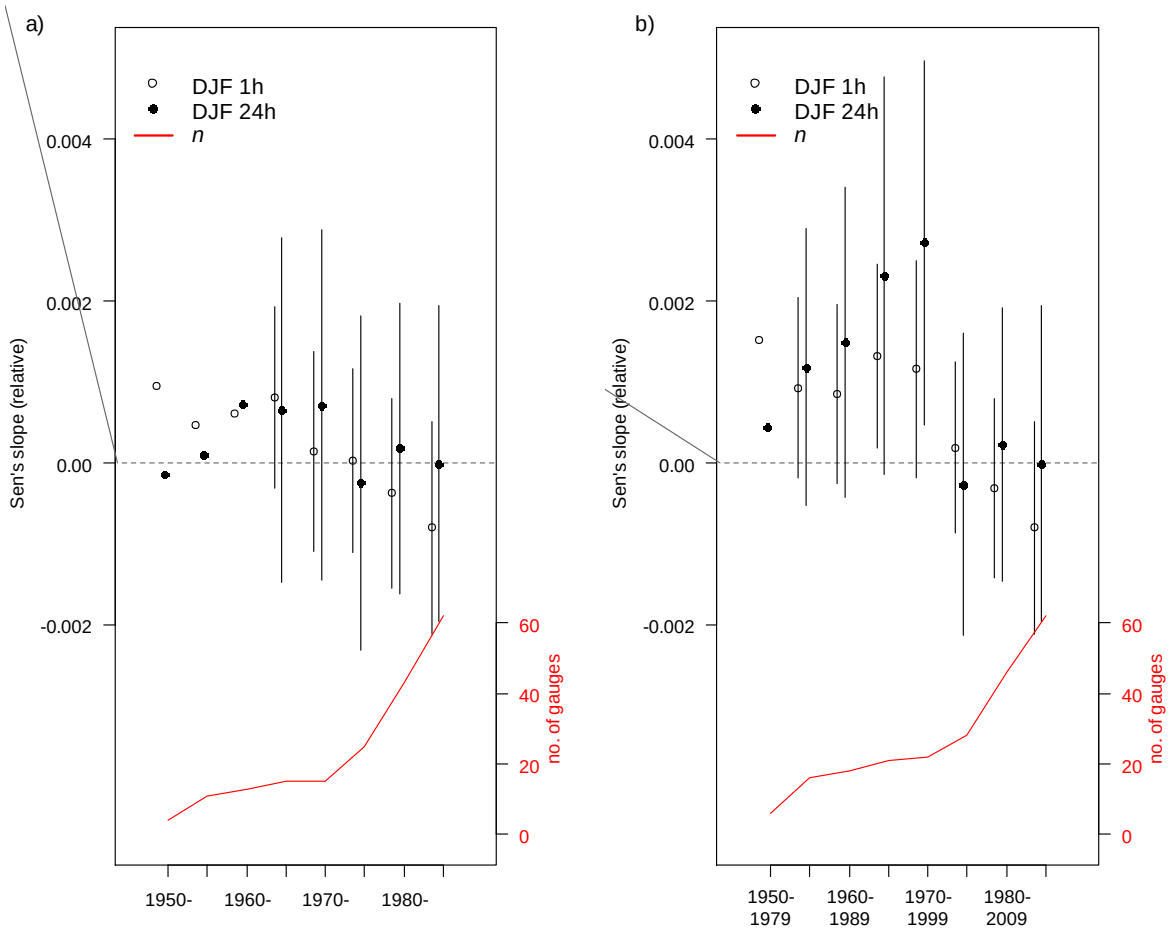

Figure 5: Relative Sen's slope (unitless) for winter (DJF) hourly and daily heavy rainfall intensity (p_{95}) in the observations for a) successive periods ending in 2014 (long trends) and b) successive 30y periods (running trends). Points show mean slope of all gauges whilst ranges show the 95% confidence interval estimated using the Student's t distribution when the number of gauges n >=15 (see Supporting Information for method details). Lower plots shows the number of gauges used for each period.

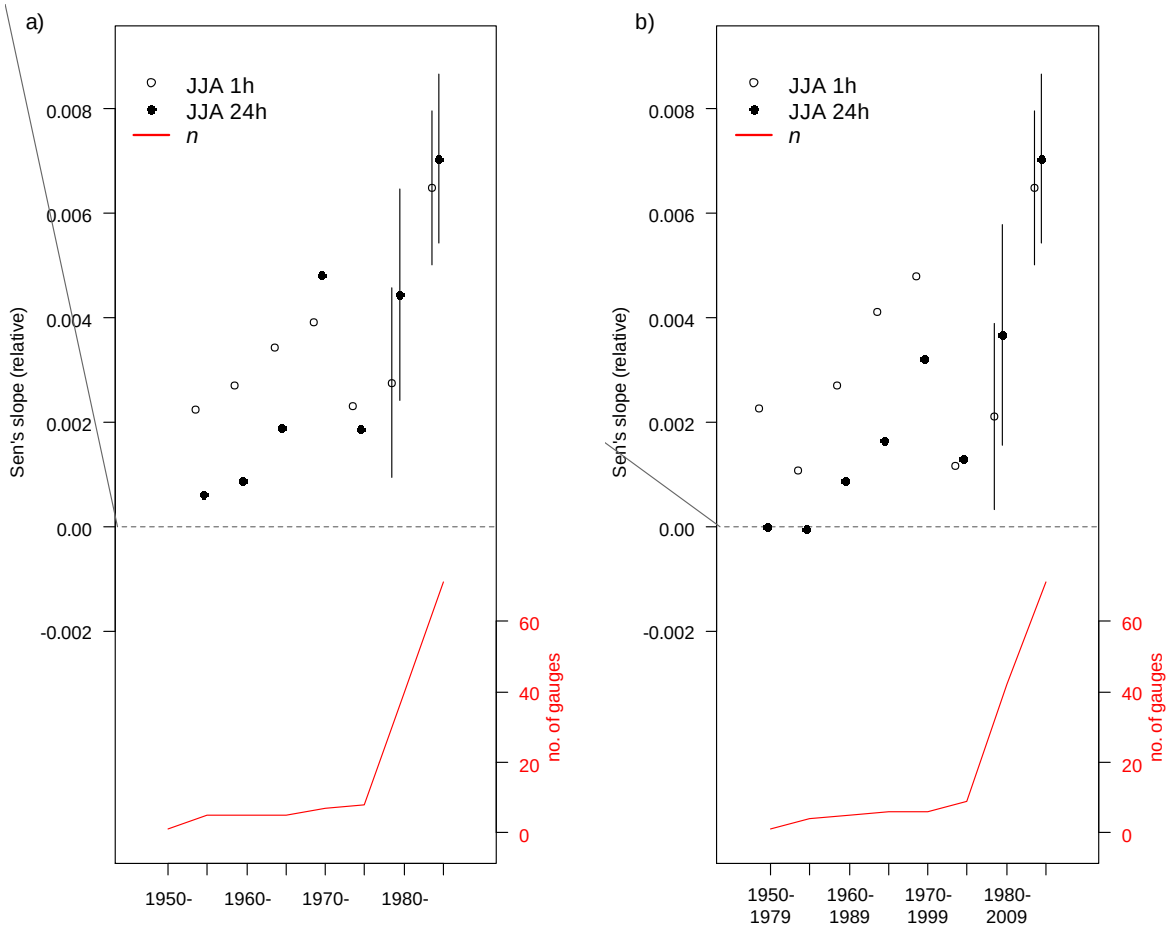

1132

1133 Figure 6: As in Figure 5 but for summer (JJA) hourly and daily heavy rainfall intensity (p_{95}) in

1134 the observations.

1135

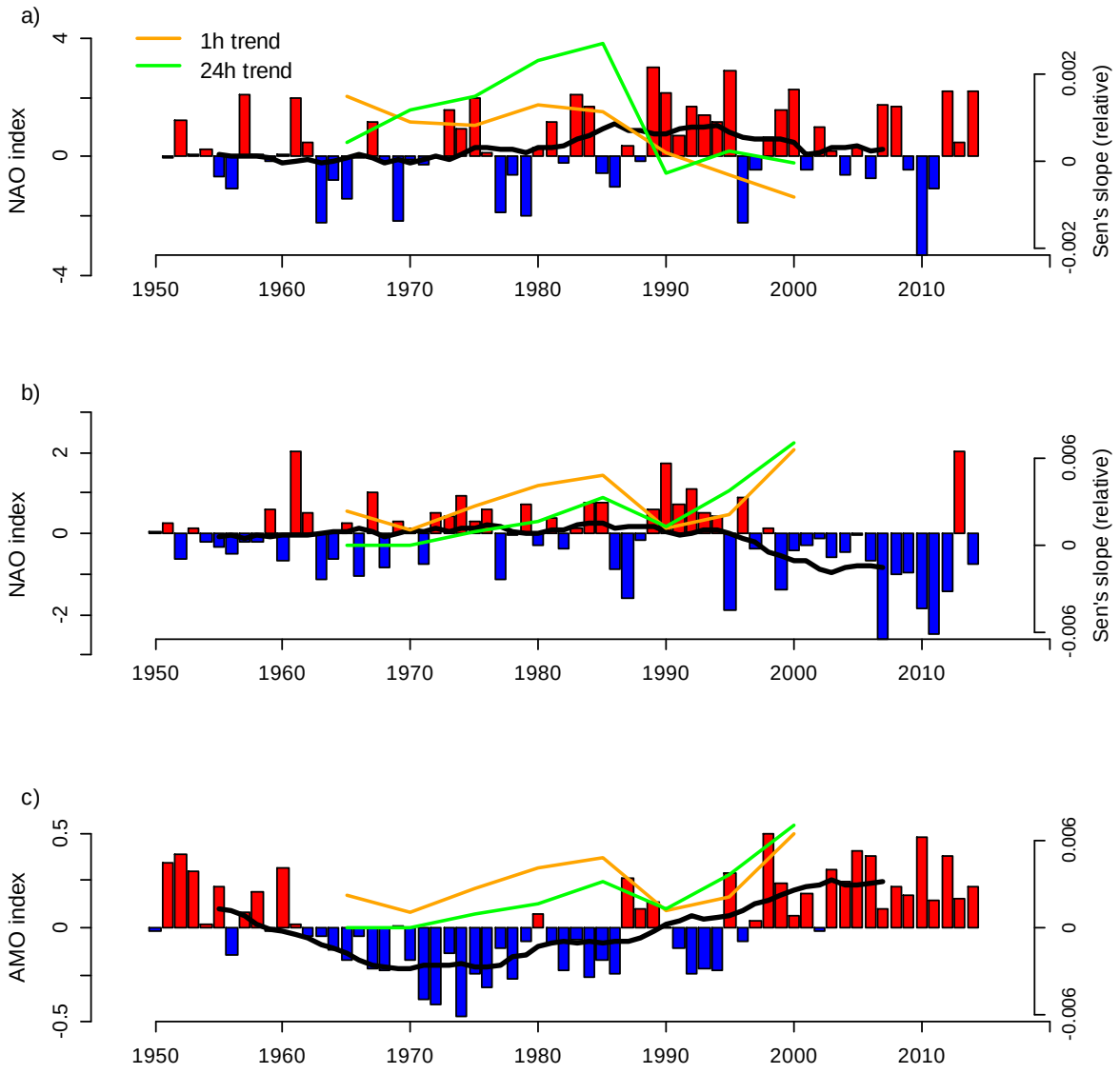

Figure 7: Time series of teleconnection indices for a) DJF NAO, b) JJA NAO, c) JJA AMO. The black line denotes the 15-year moving average. The orange and green lines indicate the mean seasonal relative Sen's slope for 1h and 24h p_{95} using running trends for each 30-year period plotted at the mid-year.

Supporting Information

Observed data homogeneity

Assessment of trends in time series may be confounded by inhomogeneities due to changes in the observing system (e.g. appearing as abrupt discontinuities or gradual changes). Abrupt discontinuities may occur due to changes in gauge relocation, instrumentation or observing and recording practices, whilst gradual changes may be a consequence of a change in gauge surroundings or in the properties of rain gauge characteristics (WMO, 2008). Several statistical tests are available to identify such discontinuities. Here we apply three such tests, the Buishand range test (Buishand, 1982), Pettit test (Pettitt, 1979) and Standard Norman Homogeneity test (Alexandersson, 1986). We consider that a series has a potential break in where at least two tests identify a significant break where the estimated year of breaks are within 5 years of each other. Aguilar et al. (2003) recommend that homogeneity tests are best performed on a time series that is expressed relative to a reference time series, i.e. one experiencing the broad climatic influences of the candidate gauge (the gauge to be tested for inhomogeneity). They suggest that inhomogeneities may be detected by comparing time series of the ratios (in the case of precipitation) or differences (for temperature) as these should show neither sudden changes, nor trends, which may be identified in a number of ways e.g. inspection of time series plots or implementation of a statistical break point test. The above tests were therefore applied to annual time series of gauge mean wet hour intensity (MWHI) expressed relative to a neighbouring gauge but only where such gauges were located no more than 25km from the candidate gauge as Blenkinsop et al. (2017) demonstrated a low correlation between gauges at greater distances, particularly in summer. As some gauges did not have any qualifying neighbouring gauges these tests were therefore also applied to annual time series of the absolute MWHI for each gauge.

The application of these tests enabled the identification of a change in resolution of some tipping bucket raingauge (TBR) measurements but due to the lack of gauge metadata (e.g. information on gauge relocation or instrument changes) it was not possible to assess other potential causes. For example, detected change points for the gauge at Upper Black Laggan (UBL), NW Scotland, matched a change in measurement resolution from 0.5mm to 0.2mm in 2003 which accounted for a decrease in mean wet hour intensity. As such changes in the resolution of measurement could affect trend analyses we corrected changes in the precision of precipitation measurement through time following Groisman et al. (2012), converting the finer-resolution measurements to the most coarse measurement for each gauge throughout the entire period of record. Under this method, small precipitation amounts are gradually accumulated until they reach the coarse resolution for each gauge. The effect of effect the change in tip resolution and subsequent homogenisation on mean wet hour intensity is illustrated in Figure S1 which shows the (MWHI) for the gauge at UBL which is contrasted with a neighbouring gauge located ~2km away. This indicates the reduction in mean intensities at UBL when the tip resolution increases

from 0.5mm to 0.2mm resulting in a Sen's statistic (i.e. trend) of -0.023, significant at the 0.01 level (panel a). After homogenisation to a consistent resolution of 0.5mm Sen's statistics is lower (-0.008), still significant at the 1% level. The influence of tip resolution is further demonstrated by comparing the original time series for Lower Black Laggan (LBL; homogeneous at 0.2mm resolution) with the higher intensities when converted to the coarser resolution as the same total rainfall is distributed over fewer wet hours. In this instance, statistical tests did not identify a break point in the original time series but all three detected a break point at the year 2000 when the UBL time series is expressed relative to that of LBL (Figure S1b). Note that the break point detection time is not expected to exactly match that of a known homogeneity given noise in the time series but here the two are broadly consistent.

Most gauges contained changes in gauge resolution (mainly 0.5mm to 0.2mm or 0.1mm to 0.2mm) although not all of these produced significant change points but were identified by changes in the time series of minimum non-zero rainfall amounts. A small number of gauges were considered unreliable and excluded on the basis of having more than one change in tip resolution. After homogenisation gauges were individually consistent at either 0.1mm, 0.2mm, 0.4mm or 0.5mm.

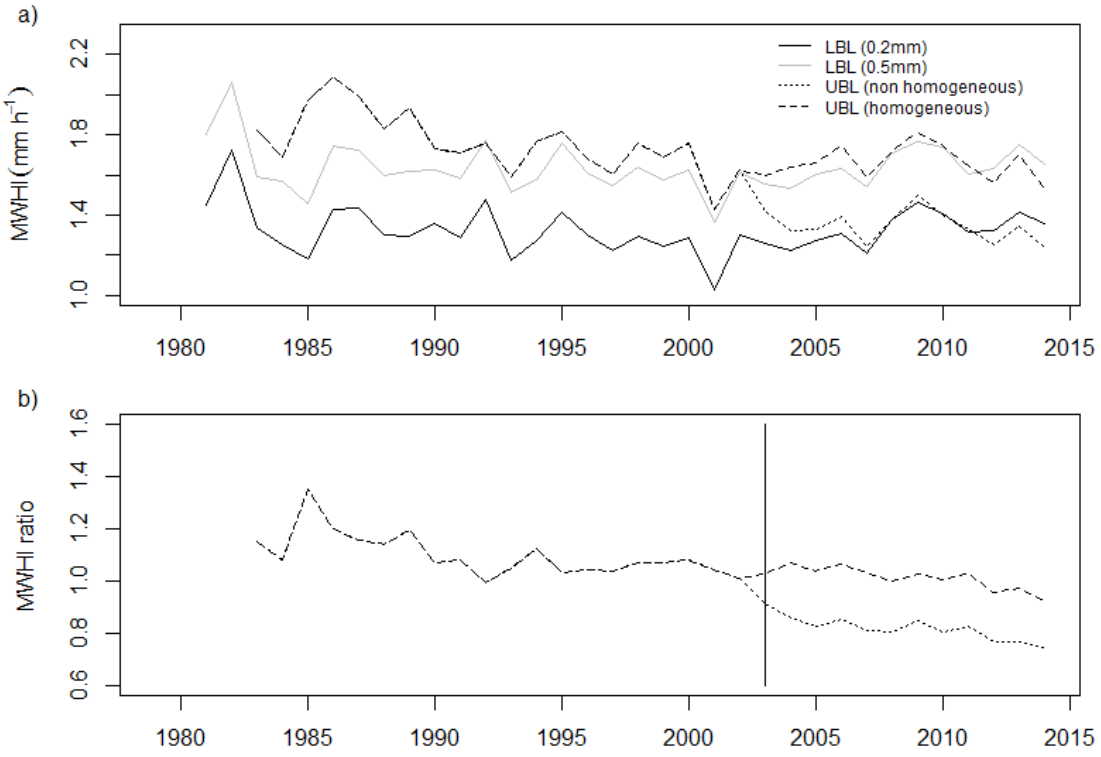

Figure S1: Time series of a) annual mean wet hour intensity (MWHI) for gauges at Lower (LBL) and Upper Black Laggan (UBL), and b) the ratio between the annual values at the two locations (UBL/LBL). Data in a) for LBL are shown using tip resolution of 0.2mm and coarsened to 0.5mm, and for UBL before and after homogenisation at the 0.5mm resolution. The ratio in b) is calculated using LBL at a resolution of 0.5mm. The vertical line denotes the timing of the change in tip resolution at UBL.

Results from observed change analysis

Additional results supporting the main text and referred to therein are provided below. The confidence intervals (CI) for the trend estimations in Figures 5 and 6 and Figures S5 and S10 are calculated using the Student's t distribution where:

$$\boldsymbol{CI = \overline{x} \pm t_{\alpha/2,df} \cdot \frac{s}{\sqrt{n}}}$$

where $\boldsymbol{\overline{x}}$ is the sample mean and $\boldsymbol{t_{\alpha/2,df}}$ is the t value associated with the required confidence level and sample size. The sample standard deviation is denoted by *s*, and the sample size by *n*.

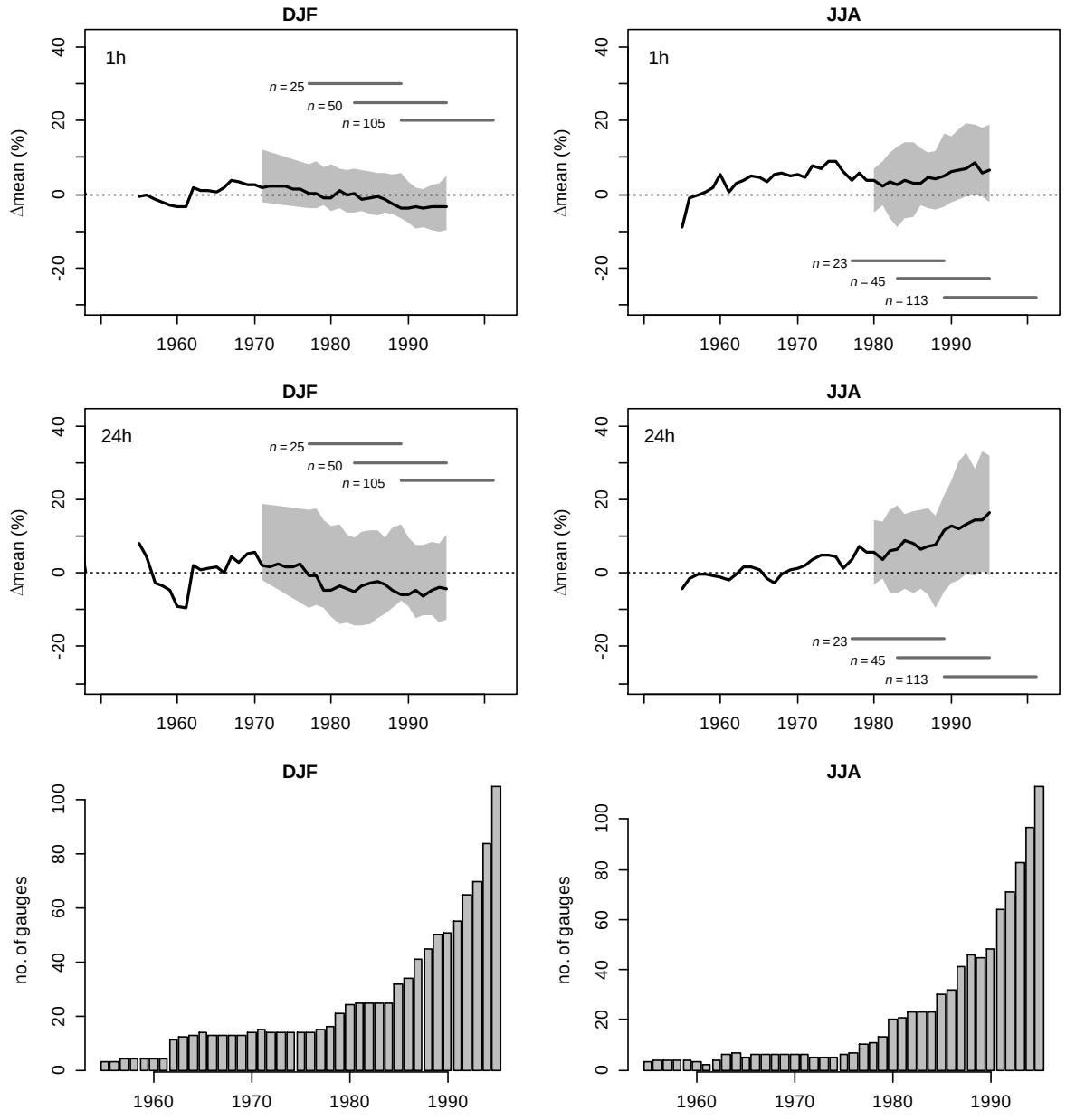

Figure S2: Percentage change in mean precipitation intensity (Δmean) for the period 2002-2014 relative to successive rolling 13-year periods in the observations (top row 1h, middle row 24h). Change is plotted at the midpoint of the earlier 13-year period. The solid line denotes the median of the change across all available gauges, the shading denotes the range bounded by the 10th and 90th percentile ranges where at least 15 gauges are available. The horizontal lines indicate the periods used to resample the observed time series to evaluate normalised change. The bar plots (bottom row) denote the number of gauges available for each period.

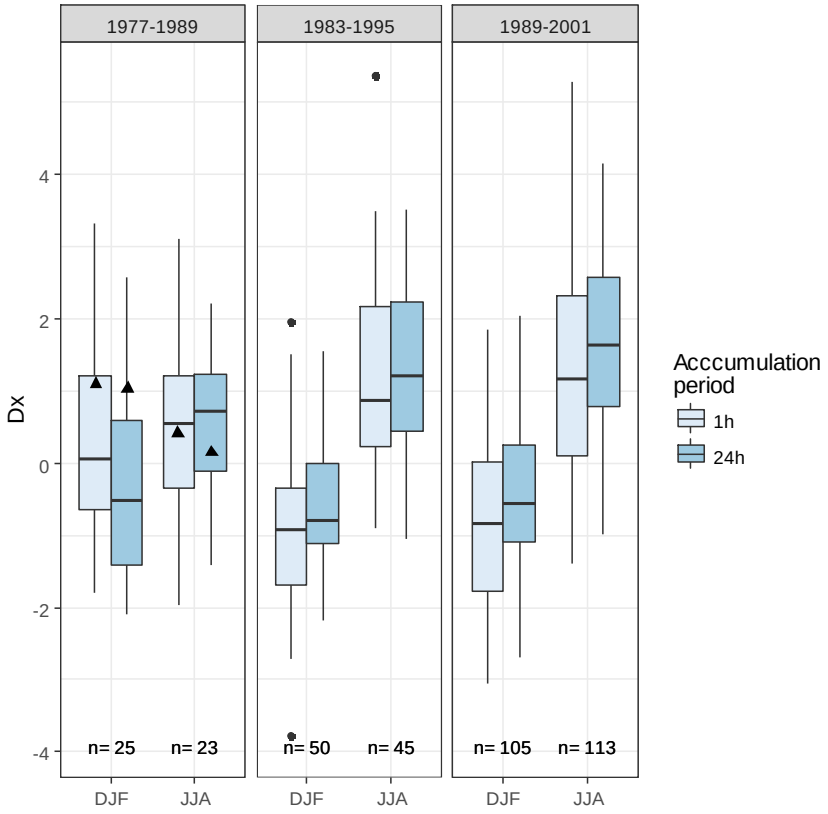

Figure S3: Distribution of normalised change in mean precipitation intensity (mean, D_x) for 1h and 24h accumulations for the period 2002-2014 relative to three 13-year periods in the observations. The black triangles denote the median of the corresponding 1.5km model results for a 25-year change (scaled linearly from the 100-year change). The value *n* denotes the number of gauges available for each period used to calculate change.

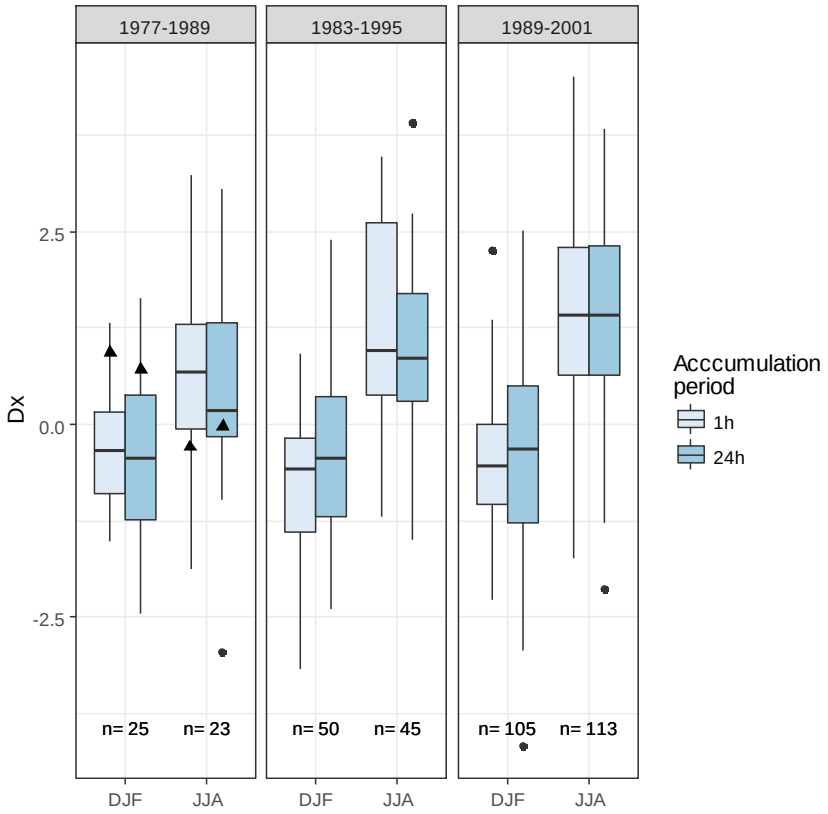

Figure S4: Distribution of normalised change in heavy precipitation (p_{99ALL}, D_x) for 1h and 24h accumulations for the period 2002-2014 relative to three 13-year periods in the observations. The black triangles denote the median of the corresponding 1.5km model results for a 25-year change (scaled linearly from the 100-year change). The value *n* denotes the number of gauges available for each period used to calculate change.

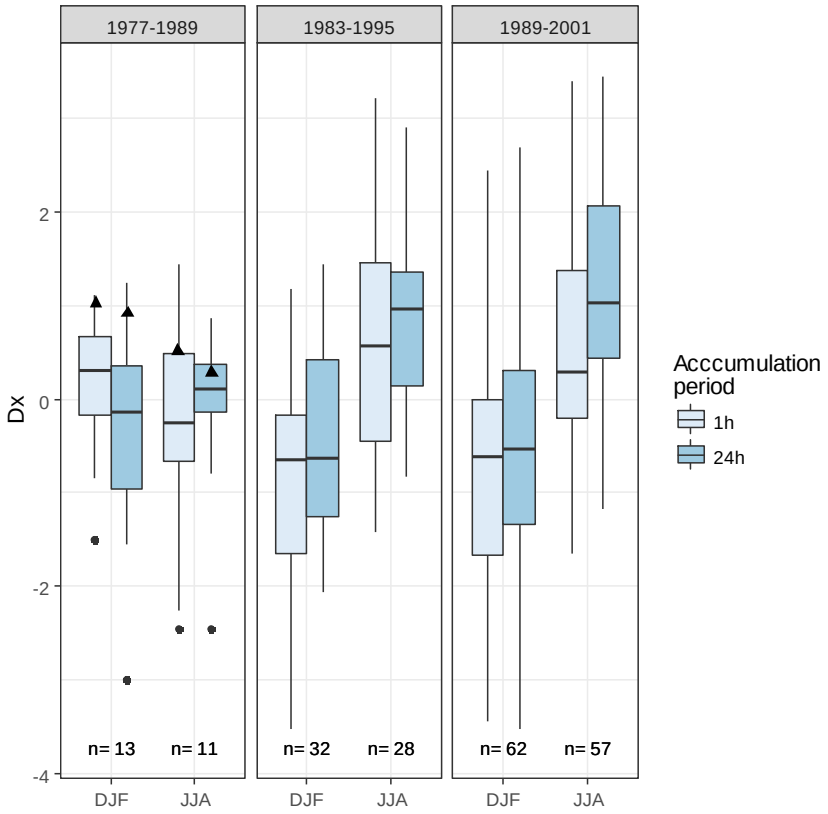

Figure S5: Distribution of normalised change in heavy precipitation intensity (p_{95}, D_x) for 1h and 24h accumulations for the period 2002-2014 relative to three 13-year periods in the observations. Here, only those gauges in the climate model domain (southern UK, see Figure 1) are used. The black triangles denote the median of the corresponding 1.5km model results for a 25-year change (scaled linearly from the 100-year change). The value *n* denotes the number of gauges available for each period used to calculate change.

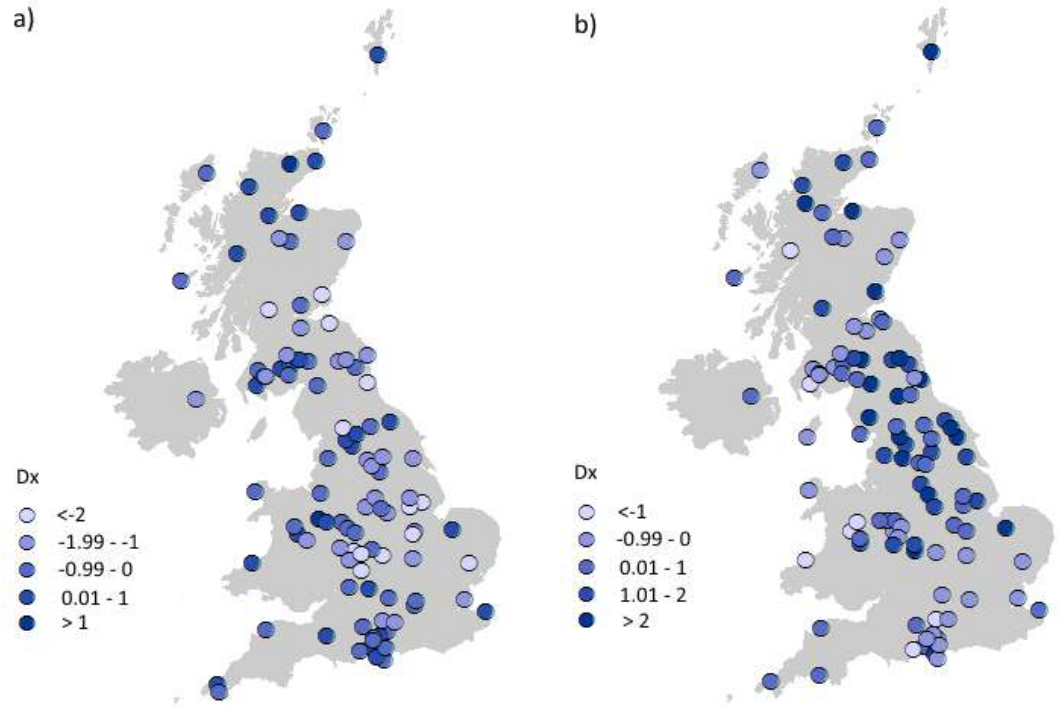

Figure S6: Spatial distribution of normalised change in heavy precipitation intensity (p_{95}, D_x) for 1h accumulations for the period 2002-2014 relative to 1989-2001 for a) DJF and b) JJA.

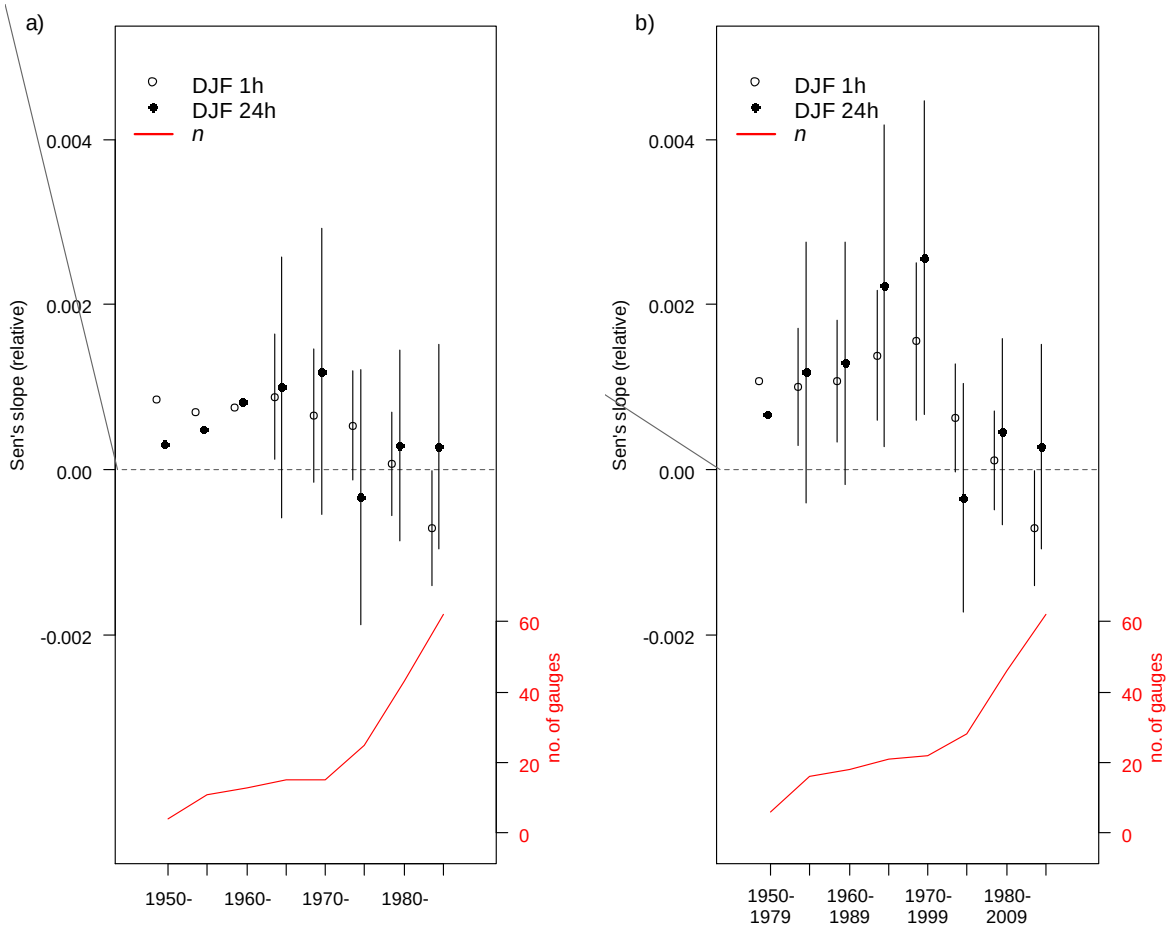

Figure S7: Relative Sen's slope (unitless) for winter (DJF) hourly and daily mean rainfall intensity for a) successive periods ending in 2014 (long trends) and b) successive 30y periods (running trends). Points show mean slope of all gauges whilst ranges show the 95% confidence interval estimated using the Student's t distribution when the number of gauges n >=15. Lower plots shows the number of gauges used for each period. See main paper for a description of the relative Sen's slope.

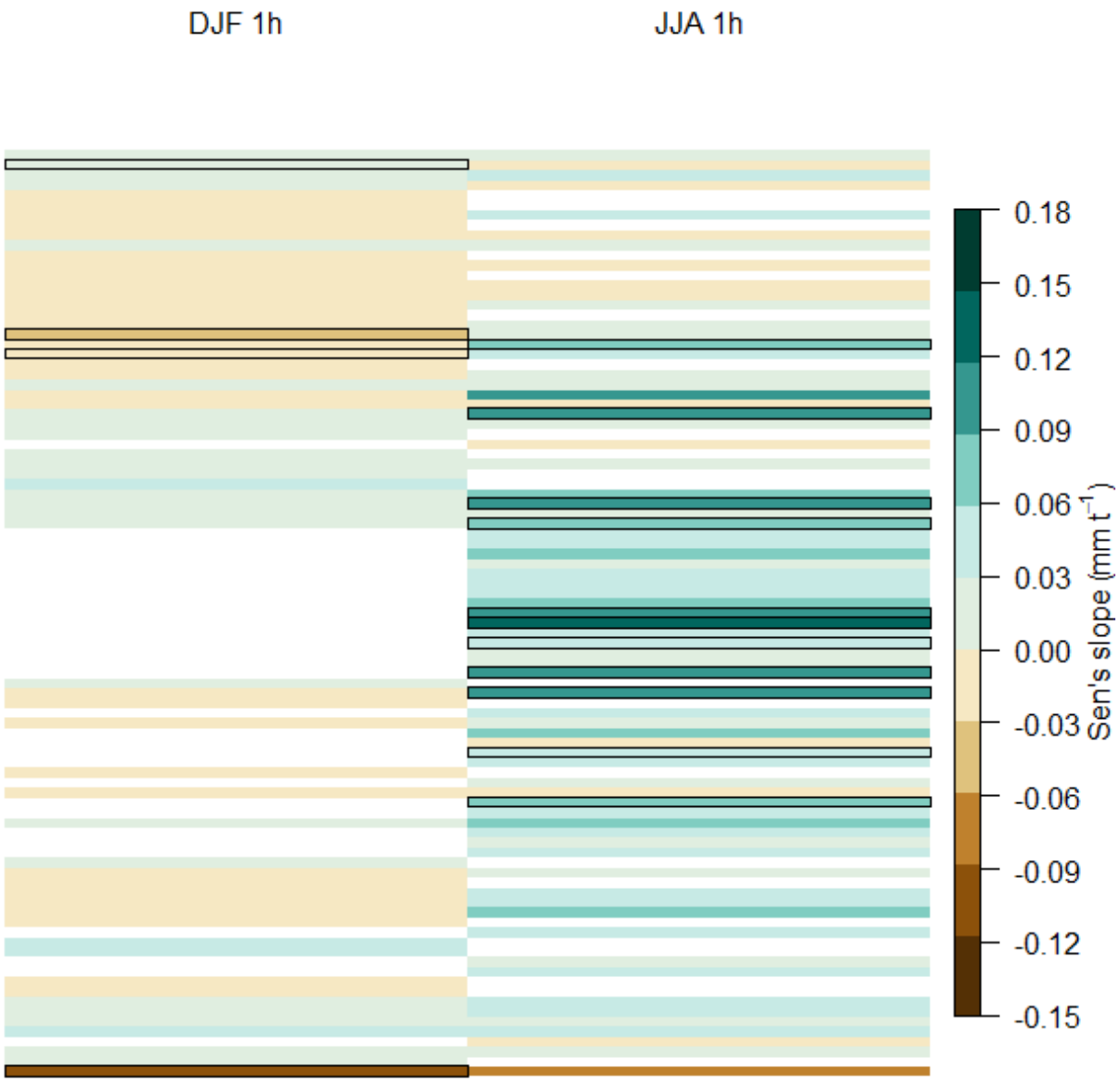

Figure S8: Sen's slope statistics (absolute) for 1h p_{95} for the period 1985-2014. Each row represents a different gauge, outlined boxes denote significance at the 95% level using the Mann-Kendall test. White areas denote gauges that do not meet completeness criteria for that season.

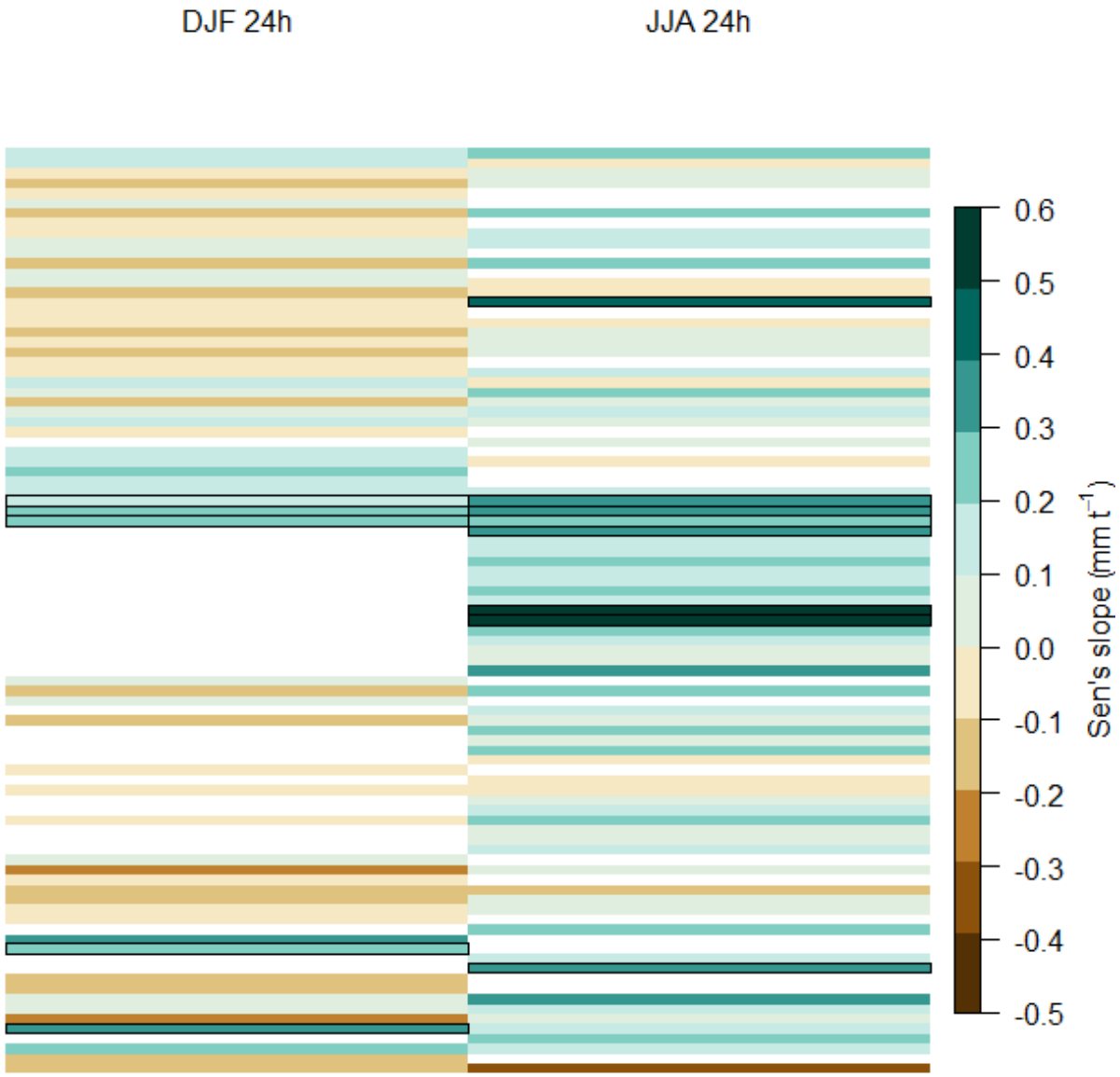

Figure S9: As in Figure S8 but for 24h p_{95}.

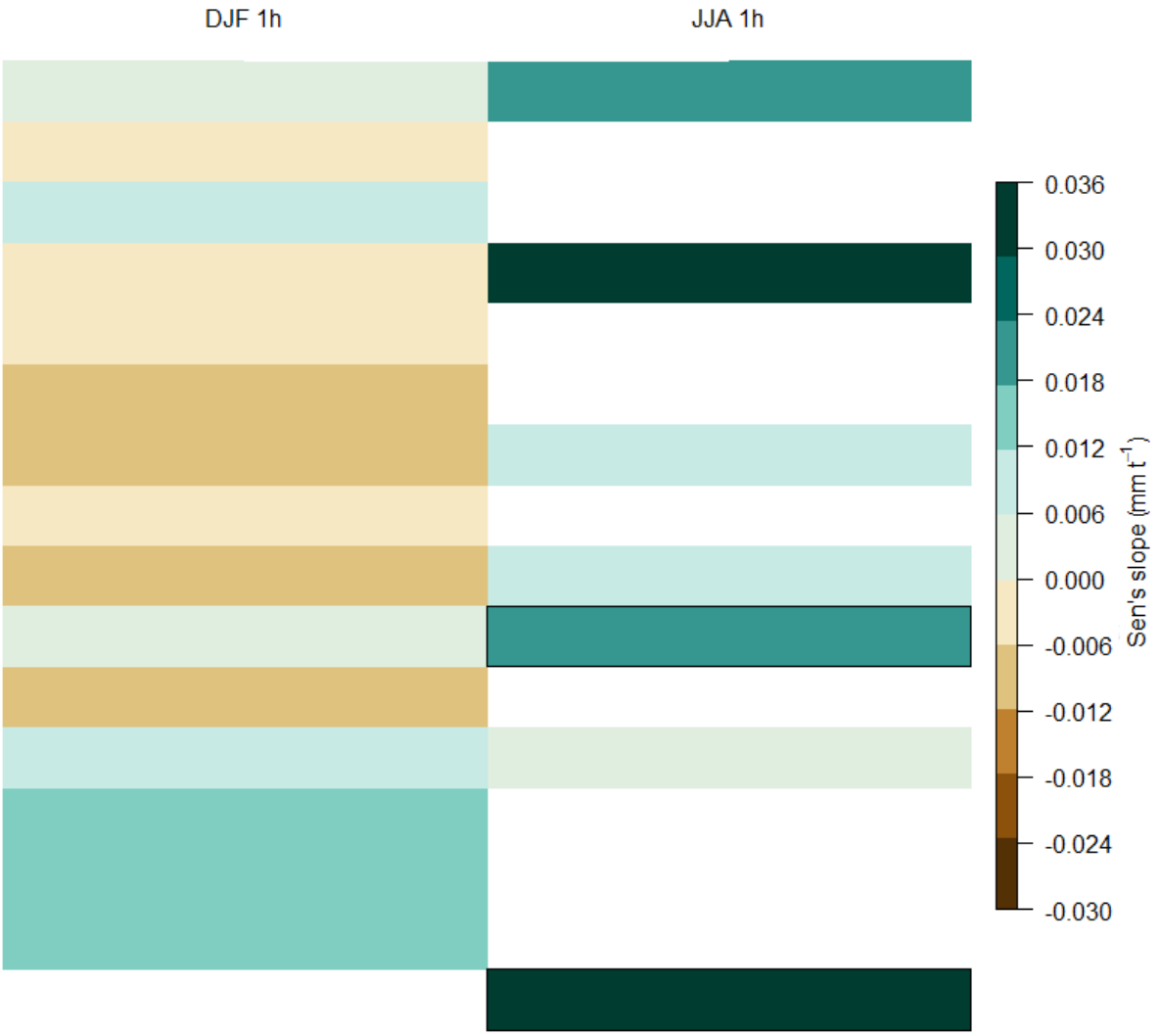

Figure S10: Sen's slope statistics for 1h p_{95} for the period 1970-2014. Each row represents a different gauge, outlined boxes denote significance at the 95% level using the Mann-Kendall test. White areas denote gauges that do not meet completeness criteria for that season.

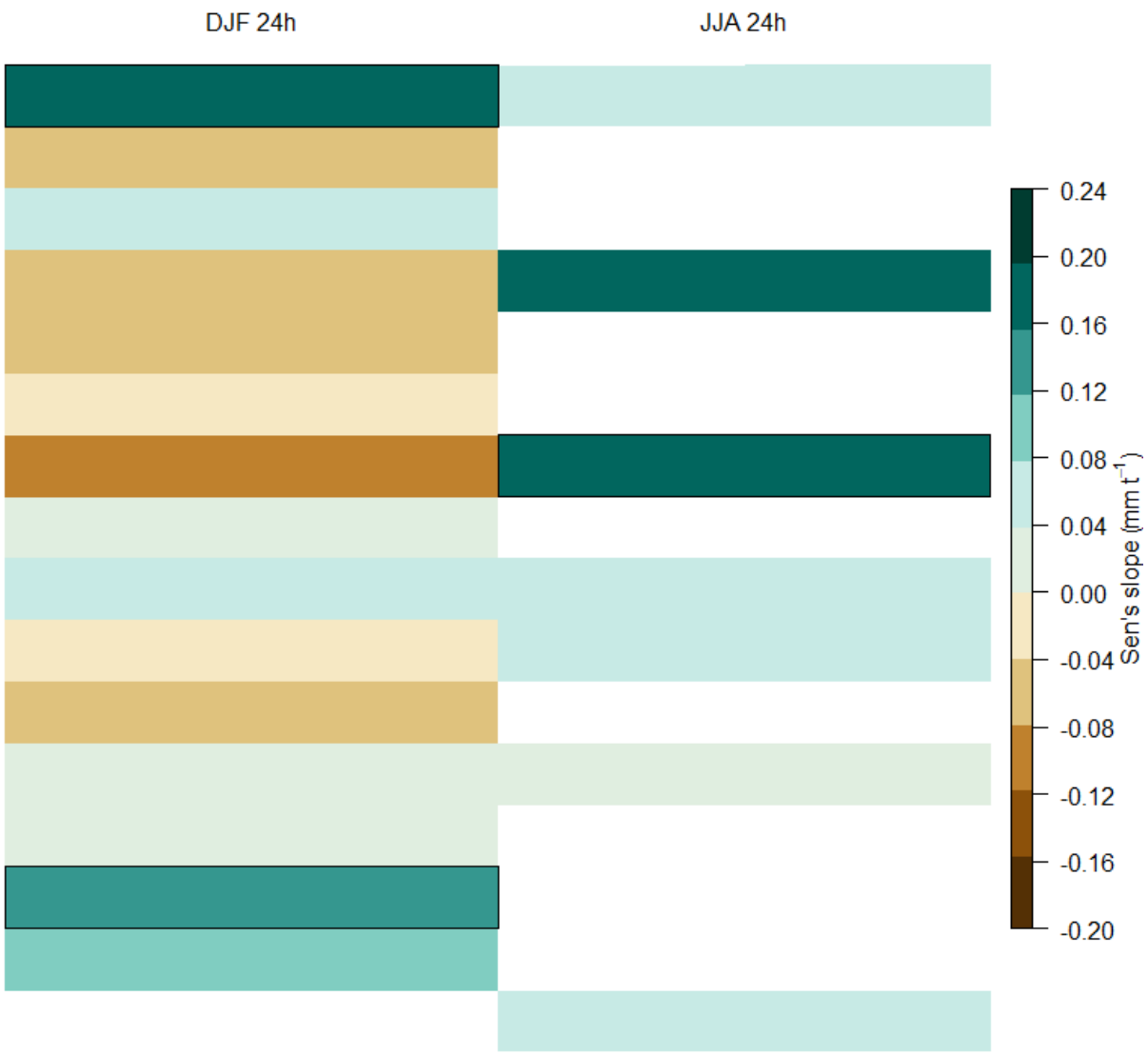

Figure S11: As in Figure S10 but for 24h p_{95}.

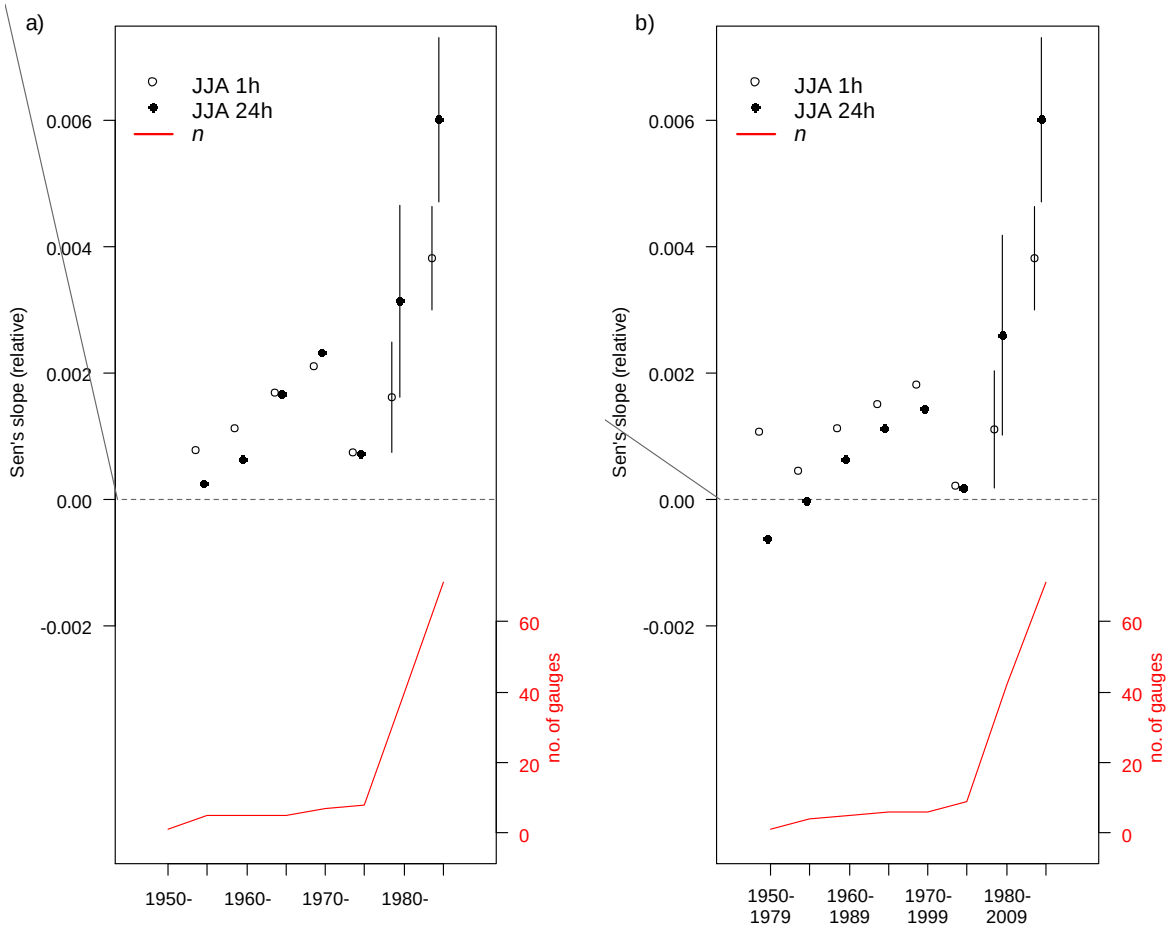

Figure S12: As in Figure S7 but for summer (JJA) hourly and daily mean rainfall intensity.

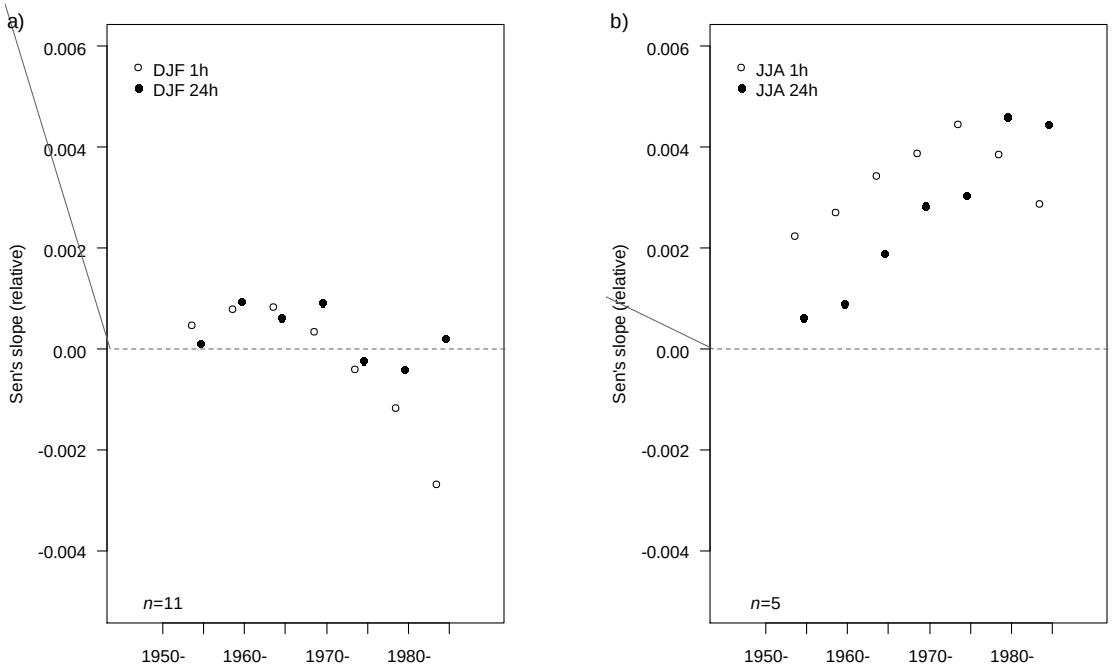

Figure S13: Relative Sen's slope (unitless) for a) winter (DJF) and b) summer (JJA) hourly and daily heavy precipitation intensity (p_{95}) for successive periods ending in 2014 (long trends). Points show mean slope using only those gauges for which trends may be calculated for all periods from 1955, *n* denotes the number of gauges. See main paper for a description of the relative Sen's slope.

Variance estimates from model and observations

Variance in 13-year heavy precipitation intensity (p_{95}) obtained by bootstrap resampling the 13 years of data in the control (future) period σ_c^2 (σ_f^2) for the model are shown below in Tables S1 and S2. Also shown are variance estimates for the observations, for the 2002-2014 period, again estimated by bootstrap resampling the 13 years of data. It can be seen that the variance estimates agree well between the observations and the model control simulation, for precipitation accumulated on both the daily and hourly timescale, which gives credibility to the noise estimation that goes into the model detection time estimates.

	1.5km	5km	12km	50km
Daily (Control)	**1.676 (0.700,4.449)**	**1.662 (0.693,4.235)**	**1.461 (0.621,3.842)**	**1.060 (0.558,2.575)**
Daily (Future)	**6.647 (2.620,21.115)**	**6.697 (2.532,20.740)**	**5.957 (2.567,19.000)**	**4.984 (2.229,16.218)**
Hrly (Control)	**0.038 (0.018,0.085)**	**0.035 (0.016,0.078)**	**0.028 (0.013,0.065)**	**0.016 (0.009,0.030)**
Hrly (Future)	**0.088 (0.036,0.258)**	**0.082 (0.034,0.236)**	**0.072 (0.028,0.196)**	**0.048 (0.016,0.107)**
Daily (Observations)	**1.554 (0.663,4.130)**	-	-	-
Hrly (Observations)	**0.043 (0.020,0.095)**	-	-	-

Table S1: Variance in 13-year heavy precipitation intensity (p_{95}) in winter (mm^2), for the control (blue) and future (red) periods, for precipitation accumulated across a range of space (1.5km-50km) and time (hrly-daily) scales. Comparable results are shown for observations (green) calculated over the period 2002-2014 but at the point scale. Shown is the median of the variance across southern UK land points, and in brackets are the 10th and 90th percentiles of the spatially varying variance estimates. Variance is calculated across 100 estimates of p_{95} obtained by bootstrap resampling the observed or model simulated precipitation time series.

	1.5km	5km	12km	50km
Daily (control)	**8.337 (3.577,22.997)**	**7.823 (3.313,22.310)**	**6.883 (3.008,21.842)**	**4.814 (2.138,11.778)**
Daily (future)	**24.245 (8.799,63.433)**	**21.355 (7.951,56.065)**	**18.272 (7.121,47.927)**	**11.051 (3.887,33.724)**
Hrly (control)	**0.364 (0.162,0.791)**	**0.301 (0.131,0.663)**	**0.220 (0.091,0.512)**	**0.095 (0.041,0.212)**
Hrly (future)	**1.528 (0.588,3.854)**	**1.090 (0.443,2.601)**	**0.665 (0.277,1.468)**	**0.210 (0.082,0.499)**
10min (control)	**0.040 (0.019,0.083)**	**0.028 (0.013,0.056)**	**0.018 (0.007,0.037)**	**0.008 (0.003,0.019)**
10min (future)	**0.172 (0.071,0.444)**	**0.093 (0.042,0.219)**	**0.046 (0.020,0.115)**	**0.013 (0.005,0.039)**
Daily (Observations)	**5.454 (2.539,13.444)**	-	-	-
Hrly (Observations)	**0.244 (0.108,0.655)**	-	-	-

Table S2: As Table S1 but for variance in 13-year heavy precipitation intensity (p_{95}) in summer (mm^2).

References

Aguilar E, Auer I, Brunet M, Peterson TC, Wieringa J, 2003. Guidance on metadata and homogenization. WMO TD N. 1186 (WCDMP N. 53); 51pp.

Alexandersson H, 1986. A homogeneity test applied to precipitation data. *International Journal of Climatology*, 6, 661-675.

Blenkinsop S, Lewis E, Chan SC, Fowler HJ, 2017. An hourly precipitation dataset and climatology of extremes for the UK. *International Journal of Climatology*, **37**, 722–740.

Buishand TA, 1982. Some methods for testing the homogeneity of rainfall records. KNMI Scientific Report WR 81-7, De Bilt, The Netherlands.

Groisman PY, Knight RW, Karl TR, 2012. Changes in intense precipitation over the central United States, *J. Hydrometeorol.*, **13**, 47–66. doi:10.1175/JHM-D-11-039.1.

Pettitt AN, 1979. A non-parametric approach to the change-point detection. Applied Statistics, 28, 126-135.

WMO, 2008. Guide to Meteorological Instruments and Methods of Observation, WMO-No. 8, Geneva, Switzerland.